https://doi.org/10.5194/acp-2021-76
Preprint. Discussion started: 5 February 2021

Atmospheric Chemistry and Physics Discussions

Isotopic Signatures of Major Methane Sources in the Coal Seam Gas Fields and Adjacent Agricultural Districts, Queensland, Australia

Xinyi Lu[1], Stephen J. Harris[1], Rebecca E. Fisher[2], James L. France[2,3], Euan G. Nisbet[2], David Lowry[2], Thomas Röckmann[4], Carina van der Veen[4], Malika Menoud[4], Stefan Schwietzke[5], Bryce F. J. Kelly[1]

[1]School of Biological, Earth and Environmental Sciences, UNSW Sydney, NSW, 2052, Australia
[2]Department of Earth Science, Royal Holloway, University of London, Egham, TW20 0EX, UK
[3]British Antarctic Survey, Cambridge, CB3 0ET, UK
[4]Institute for Marine and Atmospheric Research, Faculty of Science, Utrecht University, Utrecht, 3584 CC, the Netherlands
[5]Environmental Defense Fund, Berlin, Germany

Correspondence to: Bryce F. J. Kelly (bryce.kelly@unsw.edu.au)

Abstract. In regions where there are multiple sources of methane (CH_4) in close proximity, it can be difficult to apportion the CH_4 measured in the atmosphere to the appropriate sources. In the Surat Basin, Queensland, Australia, coal seam gas (CSG) developments are surrounded by cattle feedlots, grazing cattle, piggeries, coal mines, urban centres and natural sources of CH_4. The use of carbon ($\delta^{13}C$) and hydrogen (δD) stable isotopic composition of CH_4 can identify, distinguish between and apportion specific emissions of CH_4. However, in Australia there is a paucity of data on the various isotopic signatures of the different source types. This research examines whether dual isotopic signatures of CH_4 can be used to discriminate between sources of CH_4 in the Surat Basin. We also highlight the benefits of sampling at nighttime in warm to hot climate regions. During two campaigns in 2018 and 2019, a mobile CH_4 monitoring system was used to detect CH_4 plumes. Seventeen plumes immediately downwind from known CH_4 sources were sampled and analysed for their CH_4 mole fraction and $\delta^{13}C_{CH4}$ and δD_{CH4} signatures. The isotopic signatures of the CH_4 sources were determined using Miller–Tans plots. These new source signatures were then compared to values documented in reports and peer-reviewed journal articles. In the Surat Basin, CSG sources have $\delta^{13}C_{CH4}$ signatures between −56.0 ‰ and −51.0 ‰ and δD_{CH4} signatures between −207.0 ‰ and −193.0 ‰. Emissions from an open-cut coal mine have $\delta^{13}C_{CH4}$ and δD_{CH4} signatures of −60.3 ± 0.2 ‰ and −210.5 ± 0.5 ‰ respectively. Emissions from two ground seeps (abandoned coal exploration wells) have $\delta^{13}C_{CH4}$ signatures of −60.7 ± 0.2 ‰ and −59.9 ± 0.9 ‰ and δD_{CH4} signatures of −191.2 ± 0.5 ‰ and −185.1 ± 0.9 ‰. A river seep had a $\delta^{13}C_{CH4}$ signature of −61.1 ± 0.9 ‰ and a δD_{CH4} signature of −225.5± 1.4 ‰. Three dominant agricultural sources were analysed. The $\delta^{13}C_{CH4}$ and δD_{CH4} signatures of a cattle feedlot are −63.0 ± 1.2 ‰ and −309.0 ± 1.0 ‰ respectively, grazing (pasture) cattle have $\delta^{13}C_{CH4}$ and δD_{CH4} signatures of −59.9 ± 0.8 ‰ and −291.6 ± 2.4 ‰ respectively, and a piggery sampled had $\delta^{13}C_{CH4}$ and δD_{CH4} signatures of −47.5 ± 0.2 ‰ and −300.3 ± 1.8 ‰ respectively, which reflects emissions from animal waste. An abattoir had $\delta^{13}C_{CH4}$ and δD_{CH4} signatures of −44.3 ± 0.3 ‰ and −315.0 ± 1.3 ‰ respectively. A plume from a waste-water treatment plant had $\delta^{13}C_{CH4}$ and δD_{CH4} signatures of −47.6 ± 0.2 ‰ and −177.5 ± 1.4 ‰ respectively.

https://doi.org/10.5194/acp-2021-76
Preprint. Discussion started: 5 February 2021


Atmospheric Chemistry and Physics Discussions

In the Surat Basin, source attribution is possible when both $\delta^{13}C_{CH4}$ and δD_{CH4} are measured for the key categories of CSG, cattle, waste from feedlots and piggeries, and water treatment plants. Under most field situations using $\delta^{13}C_{CH4}$ alone will not enable clear source attribution. It is common in the Surat Basin for CSG and feedlot facilities to be co-located. Measurement of both $\delta^{13}C_{CH4}$ and δD_{CH4} will assist in source apportionment where the plumes from two such sources are mixed.

1 Introduction

If we are to achieve the goals of limiting the rise in global temperature to 2 °C as outlined in the 2015 Paris agreement of the UN Framework Convention on Climate Change (UNFCCC), we need to locate and mitigate sources of greenhouse gases due to anthropogenic industrial and agricultural activities (Nisbet et al., 2020). From measurements of the mole fraction of a gas in the atmosphere it is not possible to isolate the source of the emission, especially if many sources are juxtaposed. However, many sources of greenhouse gases have a characteristic isotopic signature, which can be used for source attribution when used in conjunction with other insights. While ethane measurements have been used previously to distinguish methane (CH_4) plumes from oil and gas activities vs. agricultural and other sources (e.g., Maazallahi et al., 2020; Mielke-Maday et al., 2019; Smith et al., 2015), the low ethane content in Australian coal seam gas (Hamilton et al., 2012; Sherwood et al., 2017) renders the use of ethane measurements for source attribution impractical. This research sought to characterise isotopic signatures and to discriminate sources of CH_4 in the Surat Basin. The study focuses on the Surat Basin, Australia, where one of the world's largest coal seam gas fields is co-located with large scale cattle feedlots. The gas fields are also surrounded by grazing cattle, piggeries, coal mines, urban centres and some natural sources of CH_4. In such regions it is a necessary but difficult task to determine how much CH_4 each sector contributes (Kille et al., 2019; Luhar et al., 2020; Mielke-Maday et al., 2019; Smith et al., 2015; Townsend-Small et al., 2015, 2016).

CH_4 is recognised as the second most abundant anthropogenic greenhouse gas species (Allen et al., 2018), contributing at least 25% of the anthropogenic radiative forcing of warming agents (including its indirect effects) throughout the preindustrial era (Myhre et al., 2013). Counting both its radiative forcing and its wider impacts, CH_4 has a global warming potential 28 to 34 times higher than carbon dioxide (CO_2) over a 100 year time span, while on a 20 year timeline CH_4 is 84 to 86 times higher than CO_2 (Myhre et al. 2013; Etminan et al., 2016). CH_4 has a lifetime of about 9 years in the atmosphere compared to CO_2, which once added to the atmosphere takes 300 to 1000 years to be cycled out of the atmosphere (Dlugokencky et al., 2011; Joos et al., 2013; Nisbet et al., 2016). For this reason, identifying and mitigating CH_4 emission provides a unique opportunity to rapidly reduce the radiative forcing of the atmosphere. The CH_4 mole fraction has been increasing since industrialisation, with a short pause between 1999 and 2006 (Schaefer et al., 2016, 2020). Since 2007, globally there has been an unremitting rise in the atmospheric CH_4 mole fraction with a further increase in the rate of growth noticeable after 2014 (Nisbet et al., 2014, 2019, 2020; Saunois et al., 2016). There is considerable debate about why CH_4 is increasing in the atmosphere, about how this methane is apportioned between natural and anthropogenic sources, and within anthropogenic sources apportionment

https://doi.org/10.5194/acp-2021-76
Preprint. Discussion started: 5 February 2021


Atmospheric Chemistry and Physics Discussions

between agriculture versus fossil fuels (Hausmann et al., 2016; Jackson et al., 2020; Kirschke et al., 2013; Nisbet et al., 2014, 2016, 2019; Rice et al., 2016; Rigby et al., 2017; Schaefer et al., 2016; Schwietzke et al., 2016; Turner et al., 2017; Worden et al., 2017). Recent ice core gas analyses of $^{14}C_{CH4}$ indicate that anthropogenic fossil fuel CH_4 emissions may have been underestimated by ~ 38 Tg to 58 Tg CH_4 per year, equivalent to ~ 25 % to 40 % of recent estimates (Hmiel et al., 2020), although this result contradicts emission estimates on the size of natural fossil fuel CH_4 sources (Etiope et al., 2019). Gas production has continuously increased every decade over the past century, and in the last decade gas production from both conventional and unconventional (shale gas, tight gas, coal seam gas) fields has increased by more than 30 % (BP, 2019). Particularly, unconventional gas is predicted to continue rising until the mid-century (DNV GL, 2019). The rapid expansion of unconventional production (EIA, 2016; IEA, 2019; McGlade et al., 2013; Towler et al., 2016) is significantly increasing CH_4 emissions (Lan et al., 2019). Thus, there is considerable interest in better quantifying CH_4 emissions from the gas sector.

In the Australian Government National Inventory reporting for various UNFCCC classifications, conventional gas data are combined with the unconventional gas data (coal seam gas), and for some categories the sub-category details are not public. For the state of Queensland, the total UNFCCC CH_4 emissions reported were 1.7 Tg of which the Oil and Natural Gas sector (1.B.2) contributed 0.16 Tg (mostly from natural gas production). This is less than the total emissions from cattle (3.A.1), which contributed 0.6 Tg (Australian Government, 2019).

Various CH_4 surveys using a vehicle mounted analyser have been undertaken in the Surat Basin (Day et al., 2015; Hatch et al., 2018; Iverach et al., 2015; Kelly et al., 2015a; Maher et al., 2014; Nisbet et al., 2020; Tsai et al., 2017). Maher et al. (2014) measured CH_4 mole fraction and stable carbon isotopic composition in the Tara region in 2012. Although elevated CH_4 mole fractions were detected within the CSG production field, no attempt was made by Maher et al. (2014) to pinpoint specific sources that caused the CH_4 enhancement. Several other mobile CH_4 surveys by Day et al. (2015), Iverach et al. (2015), Kelly et al. (2015a) and Nisbet et al. (2020) have reported high mole fractions of CH_4 measured from cattle feedlots, CSG co-produced water storage, ground seeps (abandoned exploration wells) and the Condamine River. Day et al. (2014) used a vehicle mounted CH_4 analyser to estimate CH_4 emissions from 37 well pads in Queensland (mostly from the Surat Basin) via a plume dispersion method. By performing traverses across the plume, and examining facilities using a probe attached to a CH_4 analyser, Day et al. (2014) were able to isolate and quantify emissions from well-heads, vents, pneumatic device operation and engine exhaust. The mean emission rate from well pads was approximately 0.2 kg h^{-1}. In 2015, Tsai et al. (2017) surveyed a total of 137 well pads in the Surat Basin coal seam gas field to identify and quantify CH_4 emissions. Their results show that emissions from all investigated well pads are between 0.008 kg h^{-1} and 0.4 kg h^{-1}, indicating small individual site-level emissions compared with previous studies (Brandt et al., 2016). Hatch et al. (2018) also conducted mobile CH_4 surveys north of Tara in the Surat Basin. Measurements of high CH_4 mole fraction were recorded in the region north of Dalby, but only a listing of potential sources was provided, including natural gas seeps within the Condamine River, ground seeps (abandoned gas exploration wells / uncapped water bores) or cattle feedlots. With regard to the CSG field, elevated CH_4 mole fractions

https://doi.org/10.5194/acp-2021-76
Preprint. Discussion started: 5 February 2021


Atmospheric Chemistry and Physics Discussions

were measured but further work was suggested to identify and separate the sources in this multi-source region. Iverach et al. (2015) and Nisbet et al. (2020) present data showing that there are substantial CH_4 emissions from the produced-water holding ponds (also called raw water ponds), and Nisbet et al. (2020) discuss the substantial CH_4 emissions from abattoirs in the Surat Basin. None of these past mobile CH_4 studies quantified the flux from the CSG ponds or cattle.

In the Surat Basin cattle feedlots are often located near CSG facilities as many of the feedlots are using the CSG-produced water as the water supply for the cattle (Fig 1). This makes it difficult to apportion the source of elevated CH_4 in the atmosphere from measuring CH_4 mole fraction alone. This is especially the case when measurements are not recorded close to the source, but rather from a distance, e.g., using an aerial survey. To distinguish CH_4 sources under such conditions, several studies have made use of proxy tracers such as ethane (C_2H_6), because it is often co-emitted in fossil fuel emissions (Conley et al., n.d.; Dlugokencky et al., 2011; Lowry et al., 2020; Smith et al., 2015). However, the low C_2H_6 content of the gas in the Surat Basin (<1 %; Hamilton et al., 2012) limits the usefulness of this tracer. Alternatively, the isotope composition of CH_4 ($\delta^{13}C_{CH4}$ and δD_{CH4}) can be used to assist with identifying the source of CH_4, especially when used in conjunction with atmospheric and geolocation information (Fries et al., 2018; Townsend-Small et al., 2016). Each source type of CH_4 has a representative stable isotope ratio due to different generating processes: CH_4 from microbial sources is generally depleted in both $\delta^{13}C_{CH4}$ (≈ -62 ‰) and δD_{CH4} (≈ -317 ‰) compared to thermogenic CH_4 from fossil fuel ($\delta^{13}C_{CH4} \approx -45$ ‰, $\delta D_{CH4} \approx -197$ ‰) and CH_4 derived from incomplete combustion (pyrogenic CH_4) ($\delta^{13}C_{CH4} \approx -26$ ‰, $\delta D_{CH4} \approx -211$ ‰) (Sherwood et al., 2017). Within these categories there is geographic variability in isotopic signature, caused by, for example the C3:C4 content of ruminant diets or combusted biomass (Brownlow et al., 2017; Fisher et al., 2017).

Isotope mixing models can be used for both regional and global scale studies to provide strong constraints on sources and sinks (Beck et al., 2012; Fisher et al., 2017; France et al., 2016; Lowry et al., 2020; McNorton et al., 2018; Nisbet et al., 2016, 2019; Rice et al., 2016; Rigby et al., 2017; Röckmann et al., 2016; Schaefer et al., 2016; Schwietzke et al., 2014, 2016; Tarasova et al., 2006; Turner et al., 2017; Worden et al., 2017). However, there is a wide range of reported CH_4 isotopic signatures (Sherwood et al., 2017). It is therefore important to establish suitable source signatures for the sources of interest at the regional scale. Sherwood et al. (2017) identified gaps in the isotopic characterisation in Australia. Whereas the isotopic composition of conventional fossil fuel sources is relatively well defined, there are few studies with isotope information of unconventional fossil fuels and even fewer for other CH_4 sources such as ruminants and waste. Table 1 lists literature reported isotopic signatures for typical CH_4 sources in Australia in addition to those listed in Sherwood et al. (2017), which illustrates the large variability in measured signatures across and within geographies.

Here we present mobile CH_4 surveys in the coal seam gas fields in southeast Queensland that identify and characterise major CH_4 sources. Only plumes from clearly isolated sources were sampled as detailed below. Measurements of $\delta^{13}C_{CH4}$ and δD_{CH4} from grab bag samples are then used to determine the source signature for the isolated source. These results improve the

https://doi.org/10.5194/acp-2021-76
Preprint. Discussion started: 5 February 2021

Atmospheric Chemistry and Physics Discussions

database on the isotopic chemistry of CH_4 sources in Australia, and in particular the Surat Basin. We also assess the usability of measuring just $\delta^{13}C_{CH4}$, or whether both $\delta^{13}C_{CH4}$ and δD_{CH4} are needed to differentiate between sources.

Table 1: Summary of isotopic characterisation of CH_4 sources in Australia from the literature (in addition to Sherwood et al. (2017)). NA: not applicable.

Source	$\delta^{13}C_{CH4}$ (‰)	δD_{CH4} (‰)	Reference
Fossil fuels			
Coal: Surat Basin	−68.0 to −30.3	NA	Pallasser and Stalker (2001)
Coal: Nagoorin Graben	−69.3	−203.3	Draper and Boreham (2006)
Coal: Surat Basin	−57.3 to −54.2	−215.5 to 206.7	Draper and Boreham (2006)
Coal: Bowen Basin	−51.2 to −38.6	−212.9 to −201.0	Draper and Boreham (2006)
Coal: Clarence Moreton Basin	−48.0 to −13.0	NA	Doig and Stanmore (2012)
Coal: Bowen Basin	−66.1 to −55.7	−213.0 to −223.0	Golding et al. (2013)
Coal: Surat Basin	−57.0 to −44.5	−233.0 to −209.0	Baublys et al. (2015)
Coal: Surat Basin	−64.1 to −58.6	NA	Hamilton et al. (2015)
Coal: Surat Basin	−50.8	NA	Iverach et al. (2015)
Coal: Surat Basin	−56.9 to −50.1	−210.1 to −216.3	Day et al. (2015)
Coal: New South Wales (NSW)	−52.8	−247.6	Day et al. (2015)
Commercial NG: NSW	−39.4	NA	Day et al. (2015)
Coal: Gunnedah Basin	−54.0	NA	Day et al. (2016)
Coal: Sydney Basin	−76.8 to −61.7	NA	Ginty (2016)
Coal: Sydney Basin	−66.4	NA	Zazzeri et al. (2016)
Coal: Surat Basin	−80.0 to −49.0	−310.0 to −196.0	Owen et al. (2016)
Ruminants			
Cattle: NSW	−51.0	NA	AGL Energy Limited (2015)
Cattle: Queensland	−49.0	−341	Day et al. (2015)
Cattle: NSW	−70.6	NA	Ginty (2016)
Biomass burning			
Forest: NSW	−22.2	NA	Ginty (2016)
Wetlands			
Estuary: NSW	−63.8 to −59.9	NA	Maher et al. (2015)
Freshwater swamp: NSW	−51.2	−258.6	Day et al. (2015)
Estuary: Queensland	−70.0 to −37.5	NA	Rosentreter et al. (2018)
Waste			
Landfill: NSW	−53.0	−255.2	Day et al. (2015)
Landfill: NSW	−44.0	NA	AGL Energy Limited (2015)
Landfill: Queensland	−67.4 to −49.7	−306.0 to −279.0	Obersky et al. (2018)
Anaerobic digester	−49.7	−326.2	Day et al. (2015)
Termites			
Northern Territory	−88.2 to −77.6	NA	Sugimoto et al. (1998)

https://doi.org/10.5194/acp-2021-76
Preprint. Discussion started: 5 February 2021


Atmospheric Chemistry and Physics Discussions

2 Method

2.1 Study area

The study area is situated in the Condamine region, southeast Surat Basin, and spans from Toowoomba, Dalby, Chinchilla, to Miles and the surrounding area. The size of the total study area is approximately 50,000 km^2. Figure 1 shows potential major sources of CH_4 in the study area. Location and capacity data (where available) of CSG wells, petroleum pipelines, coal mines, cattle feedlots, piggeries, landfills, wastewater treatment plants (WWTP) and abattoirs were retrieved from the Queensland Government Open Data Portal (https://www.data.qld.gov.au). CSG processing facilities and raw water ponds were manually located using Google Maps (Google LLC, USA) and Queensland Globe (Queensland Government). The locations of ground seeps discussed are a combination of those reported in Day et al. (2015) and field measurements. In Day et al. (2015) and this study, ground seeps refer not only to natural CH_4 seeps but also to abandoned exploration wells.

The Surat Basin holds more than 60 % of Australia's total proven gas reserves (Australian Competition and Consumer Commission, 2020). The study area covers many of the intensive CSG exploration and production petroleum leases (PLs). In 2018 gas was produced from 5153 exploration, appraisal and production CSG wells (Queensland Government, 2020a), as well as a small number of oil and coal exploration wells within the region (Queensland Government, 2020b). All the coal seam gas in the Surat Basin is produced from the Walloon Coal Measures (Queensland Government, 2020a). Within the region there are 42 processing facilities, 21 raw water ponds, and over 2000 km of pipelines. To the east and north of the CSG region studied there are 4 operating open-cut coal mines, and one recently closed. In total, they produced 17.5 million tonnes of saleable coal from 2018 to 2019 (Queensland Government, 2019). Coal and gas fired power stations are another potential source of CH_4. In the study area, seven power stations are operational together they account for 4.7 % of the total reported greenhouse gas emissions from the electricity sector in 2018−2019 (Australian Government Clean Energy Regulator, 2020). CH_4 sources from the agricultural sector are also considerable. Cattle and pigs are two of the most important commodities in Queensland. There are also other anthropogenic sources of CH_4 in the town areas, including landfills, wastewater treatment plants, domestic wood heaters, and automobiles, among others. Natural CH_4 seeps (the Condamine River near Chinchilla) and emissions from abandoned coal exploration wells have also been mapped within the region (Day et al., 2013, 2015; Iverach et al., 2014; Kelly et al., 2015b, 2017; Kelly and Iverach, 2016).

Ruminants such as cattle produce CH_4 in the rumen, which is then emitted to the atmosphere. A study from the Australian Commonwealth Scientific and Industrial Research Organisation (CSIRO) reported that cattle grazing is the main contributor to the total regional CH_4 emissions in the Surat Basin. Two sources of community concern, CSG and feedlots, contribute less to the regional emissions than the grazing cattle (Luhar et al., 2020).

https://doi.org/10.5194/acp-2021-76
Preprint. Discussion started: 5 February 2021


Atmospheric Chemistry and Physics Discussions

Within the Condamine Natural Resource Management Region there are ≈ 560,000 cattle (meat (feedlot and pasture) ≈ 520,000 and dairy ≈ 40,000) (Australian Bureau of Statistics, 2020). In 2018 there were 65 feedlots in the region, the largest, Grassdale Feedlot, holding up to 75,000 cattle (Beef Central, 2020; Queensland Government, 2018b). As part of this study we sampled the plume downwind of Stanbroke feedlot (Feedlot cattle in Table 2 and Fig. 3) in 2018. This feedlot has a capacity of 40,000 cattle. Most cattle in the region are in the surrounding dryland faming districts. These cattle graze a variety of crops and native grasses (we label these grazing cattle). We sampled a plume from roadside feeding grazing cattle near Dalby in 2019.

Pigs produce CH_4 via the anaerobic degradation of organic matter by bacteria in their digestive systems. Manure in the piggeries is another source of CH_4 due to processing by microbial consortia (Flesch et al., 2013). Firstly, the increasing acidogenic bacteria in the manure convert substrates into volatile fatty acids (VFAs), CO_2 and hydrogen [H]. The methanogenic bacteria then produce CH_4 from organic acids (Monteny et al., 2006). There are 67 piggeries spread throughout the Natural Resource Management Region collectively holding ≈ 270,000 pigs in 2018−2019 (Australian Bureau of Statistics, 2020). In the region, the largest piggery holds up to 142,000 pigs (Queensland Government, 2018a). In 2019 we sampled a plume downwind of the piggery called Albar Piggery, which has a registered capacity of 4,980 pigs.

Other agriculture related CH_4 emissions in the region are from urban waste biosolid and animal manure that are used to fertilise the soils in the irrigation districts and abattoirs. In Queensland there are many abattoirs that process meat for both domestic use and export. The number of abattoirs documented in the area is 20; most of these abattoirs are small, but there are two large abattoirs: Beef City (Abattoir A) and Oakey Beef Exports (Abattoir B). Beef City is one of only two comprehensive beef processing plant and feedlot operations in Australia, and one of the largest such facilities worldwide. The feedlot has a capacity of 26,500 head, and 1,134 cattle are processed in the beef processing plant per day. Oakey Beef Exports processes up to 1,200 head of cattle per day (NH Foods, 2020). Both facilities produce a range of meat and meat by-products.

Each town centre has many potential sources of CH_4 including, but not limited to, leaking gas bottles, instant hot water systems, rubbish bins, vehicles and domestic wood fires (which are common in the region). To characterise these collective emissions, samples were collected from a typical residential area in Dalby, which has a population of approximately 12,000 (Australian Bureau of Statistics, 2016).

Urban landfills are strong sources of atmospheric CH_4 (Nisbet et al., 2020). Isotopic signatures of gas emitted from landfill gas collection systems or covering soil vary depending on factors such as deposited materials, temperature, or the degree of CH_4 oxidation in the above soil layers (Zazzeri et al., 2015). As part of this study we sampled the plume downwind of the Chinchilla domestic landfill (26.74°S, 150.60°E). The landfill has a disposal area of approximately 0.07 km^2 for municipal waste and was closed to the public in 2014.

https://doi.org/10.5194/acp-2021-76
Preprint. Discussion started: 5 February 2021

Atmospheric Chemistry and Physics Discussions

Wastewater treatment plants are another source of urban CH_4 emissions, and there is a treatment plant at every major town in the region. In 2019 we sampled the plume immediately downwind of the Miles wastewater treatment plant.

Natural sources in the region include wetlands, termites, and natural fires by lightning (Lu et al., 2020). We did not attempt to characterise these natural sources as part of this study. Below we focus on the major anthropogenic sources identified in Luhar et al. (2018, 2020).

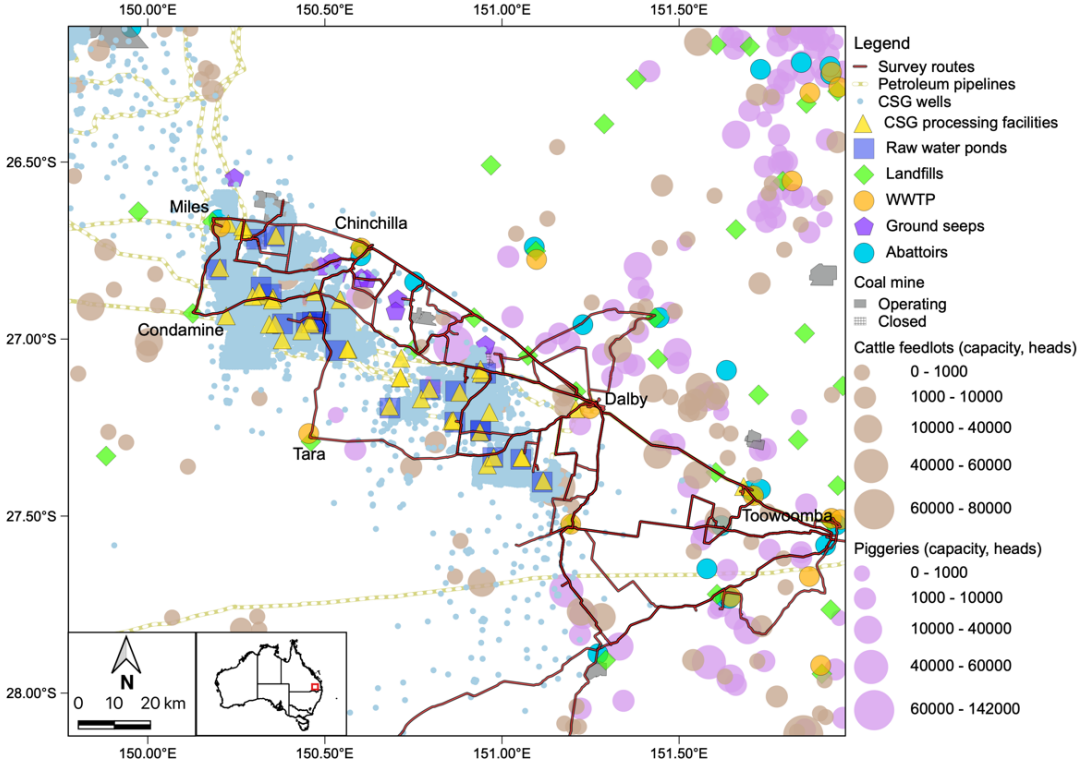

Figure 1: Map of the study area with survey routes and potential CH_4 sources. Inset map shows the location in south-eastern Queensland (Inset map data: Australian Government (2020)).

2.2 Mobile CH_4 monitoring system

To map the major CH_4 sources in the Surat Basin, we measured the CH_4 mole fraction in the atmosphere as we drove along the main roads throughout the major coal seam gas and agricultural regions of the Surat Basin. In 2018 and 2019 over 2000 km of measurements were made using a Los Gatos Research Ultraportable Greenhouse Gas Analyser (LGR-UGGA) (model 915-0011, Los Gatos Research, Inc., USA). This instrument uses off-axis integrated cavity output spectroscopy (Baer et al., 2002) and records CH_4 mole fraction data every second in parts per million (ppm) with a stated precision (1 standard deviation)

https://doi.org/10.5194/acp-2021-76
Preprint. Discussion started: 5 February 2021


Atmospheric Chemistry and Physics Discussions

of < 2 parts per billion (ppb) and a measurement range of 0–100 ppm. The air inlet was attached to a mast mounted on top of the vehicle (2.7 m above ground surface). Ambient air was then pumped into the LGR-UGGA through a Teflon tube. A Hemisphere global positioning system (GPS) (Model A326, Hemisphere GNSS, Inc., USA) was also mounted on the roof, measuring the geolocation to within 8 cm (2 standard deviations, GNSS 2017).

For a small portion of the 2018 campaign, plume mapping was done using a Picarro G2201-i cavity ring−down spectrometer (CRDS) (Picarro, Inc., USA), due to the failure of the LGR-UGGA unit. The Picarro reported precision (1 standard deviation, 30 seconds average) of CRDS for CH_4 mole fraction is 5 ppb + (0.05 % of the reading) for ^{12}C and 1 ppb + (0.05 % of the reading) for ^{13}C in high precision mode with an operational range of 1.2 to 15 ppm. Under the same operation mode, the instrument precision (1 standard deviation, 5 minutes average) for $\delta^{13}C_{CH4}$ is < 1.15 ‰ with a maximum drift (over 24 hours) of < 1.15 ‰ at 10 ppm. For the Picarro portion of the surveying we recorded the GPS location using a Kinetic Lite GPS application (Mothership Software Ltd., UK). To correct for the time lag between GPS location and CRDS recorded data caused by slow flow rate and inlet tube length (~ 2.5 m), we adjusted the time stamp of CH_4 mole fraction and $\delta^{13}C_{CH4}$ readings based on observed delay of the analyser response to a source.

One-point calibrations for the two instruments were conducted before and after each survey using Southern Ocean air provided by Commonwealth Scientific and Industrial Research Organisation (CSIRO) with a CH_4 mole fraction of 1800.6 ± 0.7 ppb and $\delta^{13}C_{CH4}$ of −47.2 ‰. The CH_4 mole fraction was measured in CSIRO's Global Atmospheric Sampling Laboratory (GASLAB) in Aspendale (Francey et al., 2003) and referenced to the World Meteorological Organization (WMO) scale (Dlugokencky et al., 2005). The calibration gas was also placed into 3 litre SKC FlexFoil PLUS sample bags (SKC Inc., USA) for shipping and analysed at the greenhouse gas laboratory of Royal Holloway, University of London (RHUL) to determine the $\delta^{13}C_{CH4}$ for the calibration air (−47.2 ± 0.05 ‰). RHUL also measured the CH_4 mole fraction (1801.2 ± 0.5 ppb), which agrees closely with the value from CSIRO, demonstrating minimal handling or gas exchange issues with the FlexFoil bags. The isotope value also closely resembles the value from flasks (−47.2 ‰) collected at Cape Grim and measured at the NOAA Global Monitoring Laboratory (White et al., 2018) around the same time as the Southern Ocean cylinder was filled by CSIRO (29 June 2016 to 11 August 2016).

2.3 Sampling and measurement methods

During the two campaigns in 2018 and 2019, driving speed was controlled between 10−80 km h^{-1} for surveys with LGR-UGGA and 10−40 km h^{-1} for surveys with Picarro G2201-i CRDS where traffic conditions are suitable. The lower driving speed coupled with real-time CH_4 mole fraction readings allowed us to detect plumes associated with potential CH_4 sources. When a constant plume was detected, we collected 10 air samples for isotopic analysis downwind of the plume by pumping air into 3 litre SKC FlexFoil PLUS sample bags with polypropylene fittings using a 2-litre medical syringe. In total, 170 air samples were collected from 17 major sources in the Surat Basin coal seam gas fields. On the day the samples were collected

https://doi.org/10.5194/acp-2021-76
Preprint. Discussion started: 5 February 2021


Atmospheric Chemistry and Physics Discussions

they were analysed for CH_4 mole fraction and $\delta^{13}C_{CH4}$ in the field using Picarro G2201-i CRDS for data quality-control purposes. The sampling of plumes favours those sources that happen to be upwind and close to a public road.

The objective of this study was not to quantify the emission rate (flux) of individual sources. Rather, our aim was to characterise the isotopic source signatures of potential significant sources of methane in the region. We did not have permission to access private properties or industrial sites, which was a significant constraint on sampling. All samples collected in this study are from publicly accessible locations. When a plume was located, we sampled several locations within the plume to maximise the range of CH_4 mole fraction values that could be obtained within the limits of public access. Sampling a large range of CH_4 mole fraction values assists with minimising the uncertainties for each source signature derived using the Miller–Tans plot method in combination with Bayesian linear regression (see Sect. 2.4).

In 2018, air samples were analysed in the greenhouse gas laboratory at RHUL for CH_4 mole fraction and $\delta^{13}C_{CH4}$ using the Picarro G1301 CRDS (Picarro, Inc., USA) and modified gas chromatography isotope ratio mass spectrometry (GC-IRMS) system (Trace Gas and Isoprime mass spectrometer, Elementar UK Ltd., UK) respectively. The Picarro G1301 CRDS was calibrated to the WMO X2004A scale using NOAA (National Oceanic and Atmospheric Administration) air standards (Dlugokencky et al., 2005; Fisher et al., 2006, 2011). For CH_4 mole fractions analysis, each sample was analysed for 210 seconds on the Picarro G1301 CRDS with a reproducibility of ± 0.3 ppb and the mean CH_4 mole fraction of the last 90 seconds of the analysis was recorded. For $\delta^{13}C_{CH4}$ analysis, samples with mole fractions above 6 ppm were diluted with zero grade nitrogen to fit the dynamic range for the GC-IRMS and then measured in triplicate on the VPDB (Vienna Pee Dee Belemnite) scale. A fourth analysis was made if the standard deviation of the first three analyses was greater than the target instrument precision of 0.05 ‰. A portion of the samples was further analysed in the Institute for Marine and Atmospheric research Utrecht (IMAU) for CH_4 mole fraction, $\delta^{13}C_{CH4}$ and δD_{CH4} using continuous-flow isotope ratio mass spectrometry (CF-IRMS) (Thermo Finnigan Delta plus XL, ThermoFinnigan MAT, Germany) (Brass and Röckmann, 2010; Eyer et al., 2016). All samples were measured directly with the automated extraction system. Most bags were sampled for 10 minutes at a flow rate of 6 mL min^{-1} for δD_{CH4} and 4 mL min^{-1} for $\delta^{13}C_{CH4}$, but samples with reported CH_4 mole fraction larger than 6 ppm by RHUL were sampled for a shorter time in order to extract a quantity of CH_4 similar to the reference air. The CH_4 from 60 mL of air was extracted for each δD_{CH4} measurement, and from 40 mL for $\delta^{13}C_{CH4}$ measurements. δD_{CH4} measurements are given on the VSMOW (Vienna Standard Mean Ocean Water) scale. A one-point calibration was done using a reference cylinder with the following assigned values CH_4 mole fraction: 1975.5 ppb, $\delta^{13}C_{CH4}$: −48.14 ‰ (VPDB), δD_{CH4}: −90.8 ‰ (VSMOW). In 2019, air samples were analysed at IMAU for CH_4 mole fraction, $\delta^{13}C_{CH4}$ and δD_{CH4} using the same CF−IRMS as 2018. Samples with reported CH_4 mole fraction larger than 3 ppm by UNSW were sampled at a lower flow rate in order to extract a quantity of CH_4 similar to the reference air. A one-point calibration was done using a reference cylinder with the following assigned values CH_4 mole fraction: 1970.0 ppb, $\delta^{13}C_{CH4}$: −48.07 ‰ (VPDB), δD_{CH4}: −88.3 ‰ (VSMOW).

https://doi.org/10.5194/acp-2021-76
Preprint. Discussion started: 5 February 2021

Atmospheric Chemistry and Physics Discussions

2.4 Data analysis

The $\delta^{13}C_{CH4}$ and δD_{CH4} for CH_4 sources of each detected plume were determined using the Miller–Tans plot approach (Miller and Tans, 2003) shown in Eq. (1):

$$\delta_{(a)} * [CH_{4(a)}] = \delta_{(s)} * [CH_{4(a)}] - [CH_{4(b)}] * (\delta_{(b)} - \delta_{(s)}) , \quad (1)$$

where $[CH_{4(b)}]$ and $\delta_{(b)}$ are the CH_4 mole fraction and $\delta^{13}C_{CH4}$ (or δD_{CH4}) of the background air, $[CH_{4(a)}]$ and $\delta_{(a)}$ are the CH_4 mole fraction and $\delta^{13}C_{CH4}$ (or δD_{CH4}) of the atmosphere and $\delta_{(s)}$ is the $\delta^{13}C_{CH4}$ (or δD_{CH4}) of the mean source, respectively. The slope of the linear regression between $\delta_{(a)} * [CH_{4(a)}]$ and $[CH_{4(a)}]$ represents the isotopic signature of the source mixed in the background ambient air. It is an adaptation of the Keeling plot method (Keeling, 1958) and avoids the need for assuming a constant background ambient air (i.e. constant: $[CH_4]$, $\delta^{13}C_{CH4}$, and δD_{CH4}). The time it takes to collect the 10 samples is approximately 30 minutes. The background air normally does not change during this period but using the Miller–Tans approach is a safeguard against any variability. For each Miller–Tans data set the linear regression line and credible intervals (analogous to confidence intervals) were determined using the PyMC3 Bayesian regression package (Salvatier et al., 2016). Bayesian regression was used since it is a robust algorithm that balances uncertainty in both the x and y axis data (Jaynes and Crow, 1999) and is suitable for small data sets (Baldwin and Larson, 2017).

3 Results and Discussion

3.1 Regional plume mapping

Two campaigns with over 2000 km routes were conducted in September 2018 and from August to September 2019 (Fig. 1). The CH_4 mole fraction in the atmosphere 2.7 m above the ground was mapped between Toowoomba and Miles (a distance of approximately 200 km. Surveys of CH_4 mole fraction during both daytime and nighttime are shown in Google Earth (Fig. 2). We shifted our focus from daytime surveying in 2018 to nighttime surveying in 2019, because during the day the sunshine heats the ground, which warms the air immediately above the surface. This causes the plumes to rise rapidly and mix with background air within the growing boundary layer, rather than accumulating within the nocturnal boundary layer. This results in daytime plumes either being missed during the mobile surveys or having a limited range of CH_4 mole fraction values. By contrast, during light to moderate wind nighttime conditions the plumes typically disperse slowly within the stable nocturnal boundary layer when there is a large temperature inversion (Stieger et al., 2015). This enabled us to sample isolated source plumes that have a greater spread of CH_4 mole fraction, which improves determination of the line of best fit in Miller–Tans plots and minimises the uncertainties of the derived isotopic source signatures. The contrast in the magnitude of the CH_4 mole fraction measured in the field between the daytime and nighttime surveys is clearly visible in Fig. 2. The distribution of the CH_4 spikes demonstrates the complex spread of the sources in the study area. Overall, measured CH_4 mole fraction ranged from 1.8 to 69.7 ppm – the highest value was recorded in a plume downwind of Oakey Beef Exports (Abattoir B).

https://doi.org/10.5194/acp-2021-76
Preprint. Discussion started: 5 February 2021

Atmospheric Chemistry and Physics Discussions

3.2 Source isotopic signatures

The results of CH_4 source signature calculations are listed in Table 2 and shown in Fig. 3. The Miller–Tans plots are shown in Figs. A1–A5 in Appendix A. All $\delta^{13}C_{CH4}$ (‰) isotopic signatures are determined with uncertainties of ± 0.2 ‰ to ± 3.4 ‰. The variability in the uncertainty is primarily due to both sampling CH_4 mole fraction range and the number of data points used in the Miller–Tans plot analysis. All δD_{CH4} (‰) signatures were determined with uncertainties of ± 0.2 ‰ to ± 4.2 ‰. The largest uncertainty was associated with the mixed urban emissions due to the limited range of sampled CH_4 mole fractions.

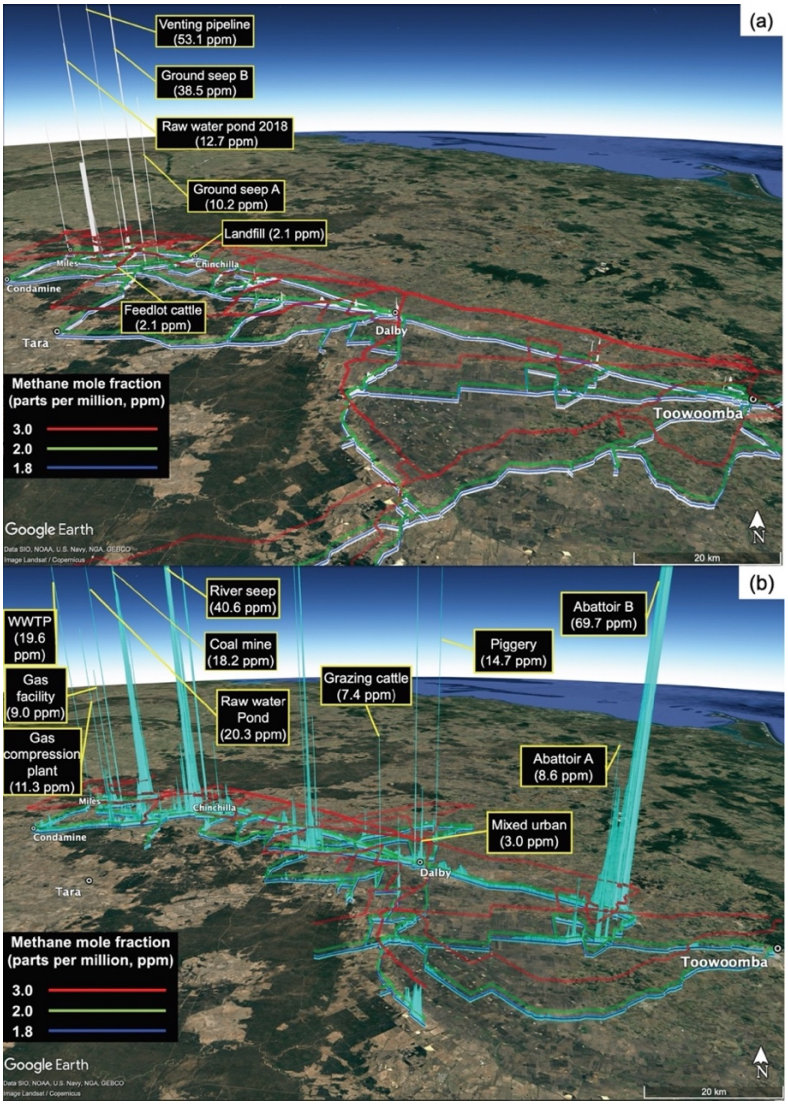

Figure 2: The vehicle mounted CH_4 survey routes throughout the Surat Basin. Daytime measurements are represented by a grey ribbon and nighttime measurements by a cyan ribbon. A linear scale is used to represent the measured CH_4 mole fraction. For all sampled plumes, the highest recorded CH_4 mole fraction is indicated (image © Google Earth).

https://doi.org/10.5194/acp-2021-76
Preprint. Discussion started: 5 February 2021

Atmospheric Chemistry and Physics Discussions

.

Table 2: CH_4 source signature results for plumes sampled in the Surat Basin 2018 and 2019 campaigns. NA: not applicable.

Upwind source	Sample date	Location (Latitude, Longitude)	Wind direction	Distance from source (km)	$\delta^{13}C_{CH4}$ (‰)	δD_{CH4} (‰)	No. of samples ($\delta^{13}C$ and δD)
CSG infrastructures							
Venting pipeline	20/9/18	26.89935° S, 150.47316° E	SW	<0.1	−54.1 ± 0.3	−199.0 ± 0.2	9 and 5
Gas compression plant	22/9/18	26.88442° S, 150.34508° E	NE	0.6	−53.5 ± 0.4	−193.1 ± 0.9	9 and 5
CSG facility	2/9/19	26.68141° S, 150.26974° E	W	0.1	−55.7 ± 0.3	−207.4 ± 1.3	6
Raw water pond (2018)	22/9/18	26.71666° S, 150.30706° E	SE	<0.1	−50.9 ± 0.9	NA	7 and NA
Raw water pond (2019)	1/9/19	26.72668° S, 150.31171° E	NW	1.0	−52.2 ± 1.1	−195.7 ± 2.1	3
Coal mining							
Coal mine	1/9/19	26.65342° S, 150.36480° E	NW	2.7	−60.3 ± 0.2	−210.5 ± 0.5	5
Ground and river seeps							
Ground seep A	19/9/18	26.78030° S, 150.52285° E	NW	<0.1	−59.9 ± 0.9	−185.1 ± 0.9	8 and 3
Ground seep B	19/9/18	26.79769° S, 150.48646° E	NW	<0.1	−60.7 ± 0.2	−191.2 ± 0.5	8 and 5
River seep	2/9/19	26.80560° S, 150.57352° E	E	0.3	−61.1 ± 0.9	−225.5 ± 1.4	4
Beef processing abattoirs							
Abattoir A	12/9/18	27.52994° S, 151.60254° E	E	1.1	−45.8 ± 0.3	NA	9 and NA
Abattoir B	4/9/19	27.42310° S, 151.70059° E	E	0.2	−44.3 ± 0.3	−315.0 ± 1.3	9
Agriculture							
Feedlot cattle	20/9/18	26.81209° S, 150.40338° E	SW	0.1	−63.0 ± 1.2	−309.0 ± 1.0	9 and 5
Grazing cattle	29/8/19	27.14643° S, 151.15916° E	NE	<0.1	−59.9 ± 0.8	−291.6 ± 2.4	6
Piggery	5/9/19	27.10768° S, 151.30661° E	NE	0.6	−47.5 ± 0.2	−300.3 ± 1.8	10
Landfill							
Chinchilla landfill	20/9/18	26.74148° S, 150.59905° E	SW	<0.1	−52.0 ± 1.0	NA	10 and NA
WWTP							
Miles WWTP	2/9/19	26.66612° S, 150.18469° E	W	<0.1	−47.6 ± 0.2	−177.5 ± 1.4	6
Other							
Mixed urban emissions	5/9/19	27.18827° S, 151.26197° E	NE	NA	−43.4 ± 3.4	−184.1 ± 4.2	9

330

https://doi.org/10.5194/acp-2021-76
Preprint. Discussion started: 5 February 2021

Atmospheric Chemistry and Physics Discussions

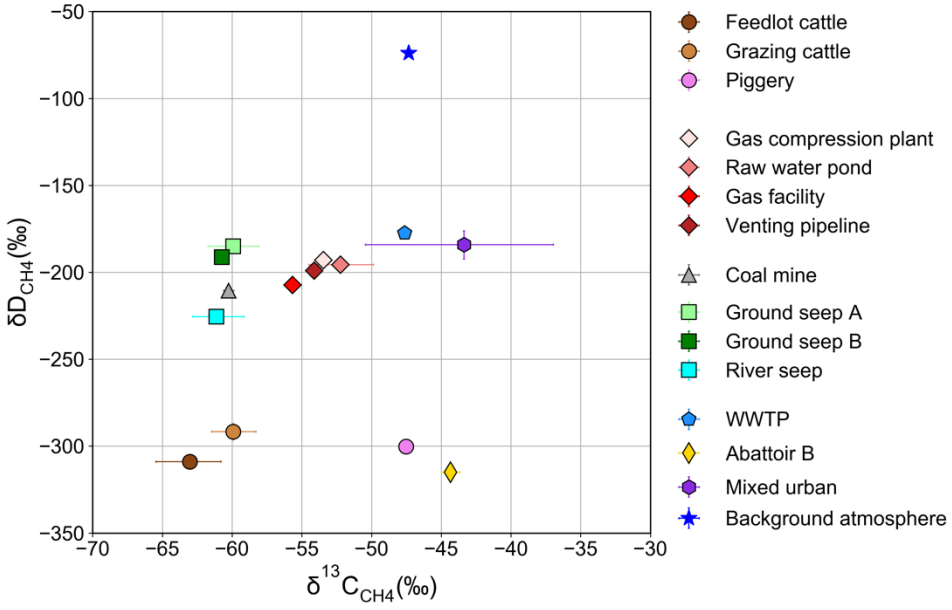

Figure 3: Dual isotope plot of all measured CH_4 sources in the study. For markers with missing error bars the uncertainties were smaller than the symbol size. Please refer to Table 2 for detailed information of plotted data.

3.2.1 Coal seam gas infrastructures

There are many portions of the CSG production and processing lifecycle where CH_4 can be released, either accidentally or by deliberate venting. CH_4 can be released intentionally at high-point vents along the produced water pipelines, outgassed from raw water ponds, or released as part of other venting or flaring operations. Unintentional CH_4 releases can occur anywhere where there are joints and seals, which can be at well heads, or along gas distribution lines, compression stations, and processing plants. The isotopic signatures of the resultant CH_4 emissions may vary depending on the origin of the gas within a gas field. The production processes and conditions of the coal and associated groundwater are not constant throughout a region, which can result in variations of the isotopic composition of the gas both spatially and with depth (Hamilton et al., 2015; Iverach et al., 2017). In the Surat Basin CSG fields, all CH_4 plumes from active CSG production and processing sources sampled show relatively little variability and sit in a distinct cluster isolated from non-CSG sources in Fig. 3. These plumes were from a range of sources including a high-point vent on a produced water pipeline, a gas compression plant, a raw water pond (measured in both 2018 and 2019 campaign), and a CSG facility (see Table 2).

Downwind of the high point vent on the produced water pipeline we sampled a plume with a maximum CH_4 mole fraction reading of 35.0 ppm (wind direction was SW) approximately 15 m from the venting point. The $\delta^{13}C_{CH4}$ and δD_{CH4} signatures of the vented gas were -54.1 ± 0.3 ‰ and -199.0 ± 0.2 ‰.

https://doi.org/10.5194/acp-2021-76
Preprint. Discussion started: 5 February 2021


Atmospheric Chemistry and Physics Discussions

Another major CSG CH_4 plume detected was associated with nighttime operations at the APLNG Talinga gas compression plant (Gas compression plant Table 2, Fig. 3). On the evening of sampling, this plume extended for 17 km (see Fig. 2). The peak CH_4 mole fraction measured was 11.3 ppm approximately 0.6 km downwind of the facility. The sampled gas had $\delta^{13}C_{CH4}$ and δD_{CH4} signatures of −53.5 ± 0.4 ‰ and −193.1 ± 0.9 ‰, respectively.

The Glen Eden raw water pond was surveyed on 22 September 2018 and 1 September 2019 (Raw water pond 2018, 2019 in Table 2, Fig. 3). This pond is one of the many in-field storages that temporarily hold water gathered from each CSG well-head (QGC, 2014). The $\delta^{13}C_{CH4}$ signatures of the gas sampled were −50.9 ± 0.9 ‰ and −52.2 ± 1.1 ‰ in 2018 and 2019, respectively, with a δD_{CH4} signature of −195.7 ± 2.1 ‰ in 2019. No significant differences were found between the $\delta^{13}C_{CH4}$ signatures from the two campaigns for this pond. The results are similar to those from a previous study in the area with a $\delta^{13}C_{CH4}$ signature of −50.8 ‰ (90 % CI, −55.7 ‰ to −45.8 ‰) from CSG water storage (Iverach et al., 2015).

In September 2019 we intersected a CH_4 plume emanating from a CSG gas transfer hub. The peak methane mole fraction measured in the plume 150 m east and downwind of the facility was 7 ppm. The $\delta^{13}C_{CH4}$ and δD_{CH4} signatures were 55.7 ± 0.3 ‰ and −207.4 ± 1.3 ‰ respectively (CSG facility Table 2, Fig. 3).

Draper and Boreham (2006) reported that the $\delta^{13}C_{CH4}$ signature for methane from the Surat Basin Walloon Coal Measures (WCM) ranged from −57.3 ‰ to −54.2 ‰, indicating secondary biogenic CH_4 with a minor thermogenic component. More recent studies by Hamilton et al. (2014, 2015) and Baublys et al. (2015) report $\delta^{13}C_{CH4}$ signature ranging from −64.1 ‰ to −44.5 ‰ with median of −52.0 ‰. These have a $\delta^{13}C_{CH4}$ range of approximately 20 ‰, while all above ground measurements fall within a narrower range. Iverach et al. (2015) and Day et al. (2015) reported $\delta^{13}C_{CH4}$ signatures from −56.9 ‰ to −50.1 ‰, and in this study we measured $\delta^{13}C_{CH4}$ signatures from −55.7 ± 0.3 ‰ to −50.9 ± 0.9 ‰ (Fig. 4). Owen et al. (2016) found that the $\delta^{13}C_{CH4}$ values for the gas reservoir (200–500 m) for coal measures in the Surat Basin were between −58.0 ‰ and −49.0 ‰. This is consistent with our study as the commercially produced gas is extracted from coal seams at depths >200 m (Queensland Government, 2020b).

The δD_{CH4} data for the WCM in the Surat Basin are relatively sparse in the literature. Early studies of the Surat Basin CSG found a range of δD_{CH4} signatures from −215.5 ‰ to −206.7 ‰ (Draper and Boreham, 2006). Baublys et al. (2015) and Day et al. (2015) reported that gas from the WCM in the same area had values from −233.0 ‰ to −209.0 ‰ and from −216.3 ‰ to −210.1 ‰. In general, the determined δD_{CH4} signatures (median = −197.4 ‰) of gas from CSG infrastructures in this study are approximately 23 ‰ less depleted than previous studies (median = −220 ‰), but fall between −310 ‰ and −196 ‰ reported by Owen et al. (2016). In Fig. 4, the data from this study are compared with $\delta^{13}C_{CH4}$ and δD_{CH4} values reported for methane sourced from coal seams worldwide (Sherwood et al., 2017). The distribution of the data from this study sit within

https://doi.org/10.5194/acp-2021-76
Preprint. Discussion started: 5 February 2021

Atmospheric Chemistry and Physics Discussions

the secondary microbial area of the CH_4 genetic diagram (see Fig. 4), which provides evidence that gas in the WCM has a secondary biogenic origin with a thermogenic component.

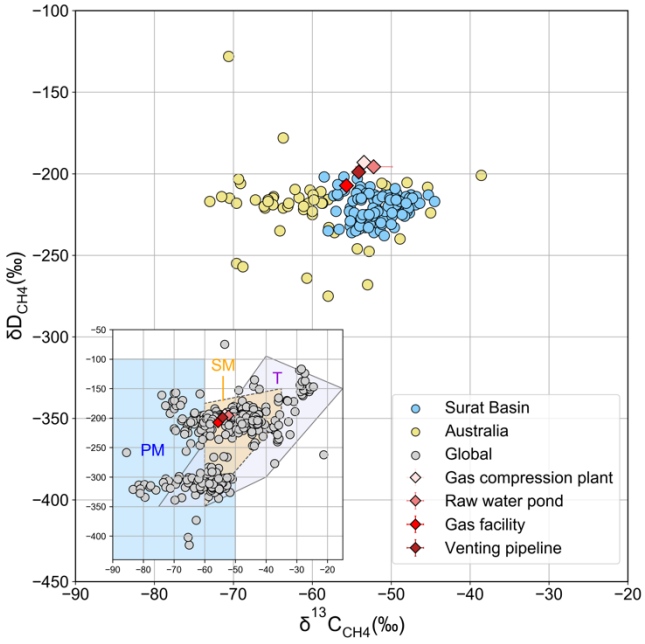

Figure 4: A comparison of $\delta^{13}C_{CH4}$ and δD_{CH4} of CSG from this study versus values from the Surat Basin, Australia wide and worldwide. Values for global measurements are shown in the inset CH_4 genetic characterisation plot. All values are taken from Sherwood et al. (2017) and literature sources listed in Table 1. The gas genetic fields are taken from Milkov and Etiope (2018). PM: primary microbial; SM: secondary microbial; T: thermogenic.

3.2.2 Coal mining

On 1 September 2019 samples were collected from a plume downwind of the Cameby Downs open-cut coal mine located approximately 16 km north-east of Miles (Coal mine in Table 2 and Fig. 3). This is one of the largest coal mines in Australia with permission to extract up to 2.8 million tonnes per annum (Mtpa) of run-of-mine (ROM) coal (Yancoal, 2018). The measured CH_4 mole fraction was between 2 ppm and 13 ppm north east of the coal mine. The sampled downwind plume from the Cameby Downs open-cut coal mine yielded $\delta^{13}C_{CH4}$ and δD_{CH4} signatures of −60.3 ± 0.2 ‰ and −210.5 ± 0.5 ‰, respectively (see Table 2). These values are close to the values measured as part of this study from the ground seeps (abandoned coal exploration wells) (see Fig. 3) and sit within the range of the global and Australian CSG sectors (see Fig. 4). These results are expected because the $\delta^{13}C_{CH4}$ signatures from coal mines depend on coal rank and the process of secondary biogenic CH_4 generation (Zazzeri et al., 2016). Coals from the Cameby Downs mine are subbituminous to high-volatile bituminous (Hamilton et al., 2014) extracted from the relatively shallow Juandah measure (<200m) in the Walloon Subgroup. Our results are consistent with the values from Owen et al. (2016), which suggests the shallow coal measures have $\delta^{13}C_{CH4}$ and δD_{CH4} signatures ranging from −80 ‰ to −50 ‰, and −310 ‰ to −210 ‰, respectively.

https://doi.org/10.5194/acp-2021-76
Preprint. Discussion started: 5 February 2021


Atmospheric Chemistry and Physics Discussions

3.2.3 Ground and river seeps

Within the Surat Basin the origin of the CH_4 associated with seeps mapped at various roadside locations or along the Condamine River west of Chinchilla is poorly characterised (Day et al., 2013, 2015; Iverach et al., 2015; Nisbet et al., 2020). In our study during the 2018 and 2019 campaigns, two ground seeps and one river seep of CH_4 were characterised (see Table 2). Both ground seeps (believed to be coal exploration wells) are located along Green Swamp Road. At each site we sampled from near the plume centre (likely over the old borehole) to approximately 50 m away downwind to obtain a spread of CH_4 mole fraction and isotopic composition data for Miller–Tans plot analysis. The peak CH_4 mole fractions measured in the bag samples from seep A and seep B were 6 ppm and 18 ppm. Seep A had $\delta^{13}C_{CH4}$ and δD_{CH4} signatures of −59.9 ± 0.9 ‰ and −185.1 ± 0.9 ‰. Seep B had $\delta^{13}C_{CH4}$ and δD_{CH4} signatures of −60.7 ± 0.2 ‰ and −191.2 ± 0.5 ‰. The two ground seeps were also investigated in previous studies made by UNSW and RHUL, which reported $\delta^{13}C_{CH4}$ of −56.9 ‰ for gas collected from seep B (Day et al., 2015) and $\delta^{13}C_{CH4}$ of −60 ‰ (Iverach et al., 2014). The isotopic signatures indicate that the gas could originate from coal seams. We were able to visually confirm pieces of historical coal exploration and it was stated in Day et al., (2015) that exploration drilling occurred at seep B during the 1970s. This is supported by the data available from the Queensland government, which shows a plugged and abandoned borehole at the same location. These likely coal seam sourced ground seeps have $\delta^{13}C_{CH4}$ and δD_{CH4} signatures that align with the more depleted biogenic values (less than 55 ‰) of global coal gas and have slightly enriched δD_{CH4} compared to Australian coal gas (see Fig. 4).

Many CH_4 seeps have been located in the Condamine River, suggesting that the emitted CH_4 is associated with coal seams in the area (Day et al., 2013; Department of Natural Resources and Mines, 2012). On 2 September 2019, we intersected CH_4 plumes near the Chinchilla weir and measured CH_4 mole fractions as high as 18 ppm in calm to light wind conditions. Gas samples had $\delta^{13}C_{CH4}$ and δD_{CH4} signatures of −61.1 ± 0.9 ‰ and −225.5 ± 1.4 ‰, respectively. These values are similar to the results from the coal mine sampled in the study area (see Fig. 3). The $\delta^{13}C_{CH4}$ value is also consistent with the results previously reported from gas samples collected in the Condamine River with values ranging from −63.4 ‰ to −59.3 ‰ (Department of Natural Resources and Mines, 2012). Iverach et al. (2017) proposed a hydrogeological conceptual model and CH_4 production evolution model between the WCM and the overlying Condamine River alluvial aquifer indicating the upward migration of CH_4 from the WCM. The relatively depleted $\delta^{13}C_{CH4}$ signature we measured is comparable to the values (−69.1 ‰) of CH_4 believed to originate from shallow WCM in Iverach et al. (2017). The $\delta^{13}C_{CH4}$ and δD_{CH4} signatures also align with the values from Owen et al. (2016) showing CH_4 from shallow coal measures (<200m) have $\delta^{13}C_{CH4}$ and δD_{CH4} signatures ranging from −80 ‰ to −50 ‰, and −310 ‰ to −210 ‰, respectively.

https://doi.org/10.5194/acp-2021-76
Preprint. Discussion started: 5 February 2021


Atmospheric Chemistry and Physics Discussions

3.2.4 Abattoirs

High CH_4 mole fractions have been observed from intensive meat processing facilities in the study area (Nisbet et al., 2020). We sampled the plumes downwind of Beef City abattoir (Abattoir A) in 2018 and Oakey Beef Exports (Abattoir B) in 2019 (see Fig. 2 and Table 2).

The highest CH_4 mole fraction measured for the Beef City was 8.6 ppm, recorded on Toowoomba Cecil Plains Road 1.3 km downwind of the complex. The Beef City plume samples yielded a $\delta^{13}C_{CH4}$ signature of −45.8 ± 0.3 ‰. Beef City is an integrated feedlot and processing plant. The measured $\delta^{13}C_{CH4}$ signature suggests that the plume sampled is most likely associated with waste emissions.

As part of the 2019 campaign, we sampled a CH_4 plume 1 km downwind of Oakey Beef Exports (Abattoir B). This plume extended northwest of the facility. The highest CH_4 mole fraction measured was 69.7 ppm, and the $\delta^{13}C_{CH4}$ signature was determined to be −44.3 ± 0.3 ‰. Emissions from Oakey Beef Exports have 4 potential sources, including a) the cattle themselves, b) emissions from anaerobic lagoons, c) emissions from biogas storage and combustion (from the facility exhaust stack), and d) by-products and animal wastes (paunch and manure). During the sampling night, smoke was observed continuously emitting from the stack associated with the main processing plant. We sampled in the centre line of that plume, but the other three potential sources must be considered, and it is likely that we sampled a mixed source plume. The processing plant is equipped with a waste-to-energy system that integrates biowaste treatment with biogas storage, processing and combustion. In the system, the biowaste is put in covered lagoons where anaerobic digestion occurs. In the anaerobic lagoons, concentrated anaerobic bacteria digest organic matter from Oakey Beef Export's biowaste to produce CH_4. During this biogas producing process, factors such as type of substrate, bacteria being used, and temperature can affect the isotopic signatures of produced gas. The generated biogas is stored in an onsite biogas storage tank and used to fuel the facility's boilers. The $\delta^{13}C_{CH4}$ signature of −44.3 ± 0.3 ‰ from this study is more enriched compared to the values from biogas plants in Heidelberg, Germany, which are fed by maize silage (−61.5 ± 0.1 ‰) and food waste (−64.1 ± 0.3 ‰) (Hoheisel et al., 2019) but close to maize-fed biogas plants in the UK (−45 ‰) (Bakkaloglu et al., 2020).

Values of $\delta^{13}C_{CH4}$ from both abattoirs are similar to values from global and Australian fossil fuels (Sherwood et al., 2017). In particular, the relatively enriched $\delta^{13}C_{CH4}$ compared to biogenic values suggests CH_4 could be derived from the incomplete combustion of biogas, which is similar with what has been reported (−48.1 ± 1.5 ‰) from measurement of a biogas power station in London, UK (Zazzeri, 2016). However, the δD_{CH4} signature of −315.0 ± 1.3 ‰ from Oakey Beef Exports indicates a biological origin. These results are comparable with that of a piggery sampled in our study (see Fig. 3), the anaerobic digester values (−326.2 ‰) reported in NSW, Australia (Day et al., 2015) and closely resemble the values from a biogas generator ($\delta^{13}C_{CH4}$ = −51.8 ± 2.4 ‰, δD_{CH4} = −305.0 ± 12.0 ‰) in Germany (Levin et al., 1993). On-site sampling at Oakey Beef Exports

https://doi.org/10.5194/acp-2021-76
Preprint. Discussion started: 5 February 2021

Atmospheric Chemistry and Physics Discussions

would be required to identify the exact source of the detected CH_4 plume. These abattoir readings highlight the problem of using just $\delta^{13}C_{CH4}$ to attribute source. Using both $\delta^{13}C_{CH4}$ and δD_{CH4} provides a more powerful discrimination between facility emissions from abattoirs and emissions from other gas sources.

3.2.5 Feedlot and grazing cattle

In the study area, we investigate the $\delta^{13}C_{CH4}$ and δD_{CH4} signatures of CH_4 emitted from Stanbroke feedlot (Feedlot cattle in Table 2 and Fig. 3) in 2018. The $\delta^{13}C_{CH4}$ and δD_{CH4} signatures determined from Miller–Tans plot had values of −63.0 ± 1.2 ‰ and −309.0 ± 1.0 ‰. The peak CH_4 mole fraction recorded was 3.2 ppm. In 2019 we sampled the CH_4 plume emitted from over 200 cattle grazing along the roadside between Dalby and Ranges Bridge (Grazing cattle in Table 2 and Fig. 3). The cattle were spread from immediately adjacent to the roadside to over 100 m away. The maximum CH_4 mole fraction value recorded for the grazing cattle plume was 7.4 ppm, and the $\delta^{13}C_{CH4}$ and δD_{CH4} isotopic signatures were −59.9 ± 0.8 ‰ and −291.6 ± 2.4 ‰, respectively.

The isotopic signature of the cattle-produced CH_4 varies depending on the diet (Levin et al., 1993). In Queensland the typical cattle diet is predominantly C4 plant with forage, grain and supplements (McGinn et al., 2008). Specifically, due to differences in diet, the $\delta^{13}C_{CH4}$ and δD_{CH4} signatures of cattle in the Surat Basin are in between the values from Levin et al. (1993) ($\delta^{13}C_{CH4}$ = −55.6 ± 1.4 ‰, δD_{CH4} = −295.0 ± 10.0 ‰, 60 – 80 % C4 diet) and Bilek et al. (2001) ($\delta^{13}C_{CH4}$ = −70.6 ± 4.9 ‰, δD_{CH4} = −358.0 ± 15.0 ‰, 90 % C3 diet) (see Fig. 5). Compared to studies in the US, $\delta^{13}C_{CH4}$ signatures in our study are more depleted than those from cattle in Townsend-Small et al. (2015) ($\delta^{13}C_{CH4}$ = −56.3 ‰, δD_{CH4} = −283.0 ‰, unspecified diet) and Townsend-Small et al. (2016) ($\delta^{13}C_{CH4}$ = −56.2 ‰, δD_{CH4} = −302.0 ‰, unspecified diet) (see Fig. 5). Both the feedlot and grazing cattle signatures determined as part of this study are generally consistent with values for ruminants around the globe and in other areas of Australia (see Table 1).

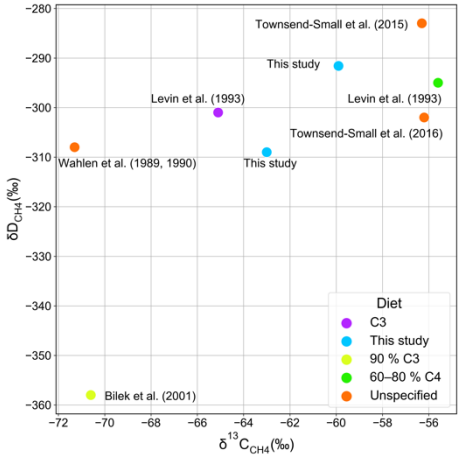

Figure 5: A dual isotope plot comparing the $\delta^{13}C_{CH4}$ and δD_{CH4} for cattle from this study with the values reported in the literature (indicated next to the data points).

https://doi.org/10.5194/acp-2021-76
Preprint. Discussion started: 5 February 2021


Atmospheric Chemistry and Physics Discussions

3.2.6 Piggery

A CH_4 plume was sampled 600 m downwind of Albar Piggery in 2019. This plume had a distinctive smell and a warmer temperature compared to the surrounding ambient air, indicating that the piggery was heated. The maximum CH_4 mole fraction measured was 14.7 ppm, and the $\delta^{13}C_{CH4}$ and δD_{CH4} signatures were −47.5 ± 0.2 ‰ and −300.3 ± 1.8 ‰, respectively (Table 2 and Fig. 3). These $\delta^{13}C_{CH4}$ and δD_{CH4} signatures are close to those reported by Levin et al. (1993) in Germany for lower pile of manure ($\delta^{13}C_{CH4}$ = −45.5 ± 1.3 ‰ and δD_{CH4} = −297.0 ± 6.0 ‰). The $\delta^{13}C_{CH4}$ and δD_{CH4} values also closely resemble our results from the abattoirs (Fig. 3).

3.2.7 Landfill

Gas samples collected downwind of the Chinchilla landfill had a CH_4 mole fraction range from 1.8 to 2.1 ppm, and a Miller–Tans plot best fit $\delta^{13}C_{CH4}$ value of −52.0 ± 1.0 ‰ (Table 2 and Fig. 3). In general, the determined $\delta^{13}C_{CH4}$ value in this study falls into the range of international and Australian CH_4 sourced from waste (Fig. 6). The isotope ratio of CH_4 in this landfill is less depleted than the mean values reported (−56.5 ‰ for surface and −58.7 ‰ for waste) of the active landfill in Ipswich, Queensland (Obersky et al., 2018) and those reported from Europe (Hoheisel et al., 2019; Xueref-Remy et al., 2020; Zazzeri et al., 2015) possibly due to CH_4 oxidation by aerobic bacteria in cover soils. Similarly, relatively enriched $\delta^{13}C_{CH4}$ values were also identified from older, closed landfills in the UK (Bakkaloglu et al., 2020; Lowry et al., 2020). Our result also closely resembles the value measured by Day et al. (2015), who reported −53.0 ‰ for a landfill in New South Wales, Australia and results from the upper layers of waste (−52.0 ‰) in Germany (Levin et al., 1993).

3.2.8 Wastewater treatment plant (WWTP)

On 2 September 2019 we sampled a plume immediately adjacent to the Miles wastewater treatment plant along Waterworks Road. This plume had a maximum CH_4 mole fraction reading of 19.6 ppm, and $\delta^{13}C_{CH4}$ and δD_{CH4} signatures of −47.6 ± 0.2 ‰ and −177.5 ± 1.4 ‰ (Table 2 and Fig. 3), respectively. In Australia the $\delta^{13}C_{CH4}$ of CH_4 emissions from the waste sector ranges from −58.8 ‰ to −44.0 ‰ with a median of −50.4 ‰ (AGL Energy Limited, 2015; Day et al., 2015; Obersky et al., 2018; Sherwood et al., 2017), the $\delta^{13}C_{CH4}$ −47.6 ± 0.2 ‰ determined for the Miles wastewater treatment plant is consistent with past results. However, the $\delta^{13}C_{CH4}$ signature is less depleted than the wastewater treatment plant values of −51.3 ± 0.2 ‰ measured in Heidelberg, Germany (Hoheisel et al., 2019), −52.3 ‰ in Cincinnati, USA (Fries et al., 2018) and −59.2 ‰ to −50.7 ‰ in London, UK (Zazzeri, 2016) for anaerobic treatment systems. The result is similar to the measurements made by Townsend-Small et al. (2012) from two wastewater treatment plants (−46.3 ‰ and −47 ‰) in the metropolitan area of Los Angeles, USA and result from aerobic digestion tank of WWTP (−45.5 ‰) in Tokyo, Japan (Toyoda et al., 2011). Both Townsend−Small et al. (2012) and Fries et al. (2018) found a more depleted δD_{CH4} for wastewater treatment plants in Los Angeles (−298 ‰) and Cincinnati (−325 ‰) compared to our result. Toyoda et al. (2019) suggested that the relatively enriched $\delta^{13}C_{CH4}$ signature could be due to aerobic digestion. A better understanding of the CH_4 from wastewater treatment plants,

https://doi.org/10.5194/acp-2021-76
Preprint. Discussion started: 5 February 2021


Atmospheric Chemistry and Physics Discussions

especially for different treatment processes (anaerobic or aerobic), in Australia is needed as it is proven to be a nonnegligible source of CH_4 emission in urban areas.

3.2.9 Mixed urban emissions

Samples from the town centre of Dalby were collected to measure their $\delta^{13}C_{CH4}$ and δD_{CH4} signatures on 5 September 2019 (Table 2 and Fig. 3). The sample location was in a park with no immediately adjacent visible sources of CH_4. At the time of sampling smoke from domestic wood fires was discernible in neighbouring areas. Results derived from Miller–Tans plots gave values of −43.4 ± 3.4 ‰ and −184.1 ± 4.2 ‰ respectively for $\delta^{13}C_{CH4}$ and δD_{CH4} with large uncertainties (Fig. 3). The signatures are believed to be a mixture of background air and wood fire smoke. Contributions from urban gas leaks may also be a component. Further investigation is needed for a better understanding of the urban emissions.

3.3 Discriminating between isotopic signatures from various sources: uniqueness and overlaps.

Various studies have pointed out that there are large overlaps in CH_4 isotopic signatures, compromising the use of isotopic constraints in models estimating CH_4 emissions (Feinberg et al., 2018; Milkov and Etiope, 2018; Sherwood et al., 2016, 2017). Figure 6 displays probability distributions of $\delta^{13}C_{CH4}$ and δD_{CH4} for fossil fuel and modern microbial processes (with their respective subcategories) in Australia (Table 1 and Sherwood et al., 2017) and around the globe (Sherwood et al., 2017). Global coal gas $\delta^{13}C_{CH4}$ has a bimodal distribution and a relatively wide range spanning from −85.5 ‰ to −16.8 ‰. In Australia, coal gas has a unimodal distribution of $\delta^{13}C_{CH4}$ ranging from −76.8 ‰ to −30.3 ‰ with a more depleted median of −54.3 ‰ due to high amount of microbial gases. Almost half of the widely spread values of coal gas have a range that overlaps with the distributions of other microbial processes. Specifically, global $\delta^{13}C_{CH4}$ of cattle varies from −71.3 ‰ to −50.3 ‰ with a median of −66.5 ‰; values for Australia range from −70.6 ‰ to −49.0 ‰ with a median of −61.5 ‰. The more enriched isotopic values found in Australian cattle are likely due to higher proportions of a C4 diet (Levin et al., 1993; McGinn et al., 2008) in these tropical herds, raised on C4 grasslands and with maize supplements.

In this study, $\delta^{13}C_{CH4}$ signatures determined from CSG processing and production infrastructures and seeps varied from −61.1 ‰ to −50.9 ‰ with a median of −55.7 ‰. This range is far narrower than the global distribution of $\delta^{13}C_{CH4}$ from coal presented in Sherwood et al. (2017) (Fig. 6), or those determined from gas and water well measurements (Baublys et al., 2015; Hamilton et al., 2014, 2015). The median of CSG $\delta^{13}C_{CH4}$ signature is about 6 ‰ more enriched than the $\delta^{13}C_{CH4}$ signature of the cattle (which ranges from −63.0 ‰ to −59.9 ‰) and about 8 ‰ more depleted than that of waste (which ranges from −52.0 ‰ to −47.6 ‰). These similar or overlapping $\delta^{13}C_{CH4}$ values for different sources mean that in areas with multiple sources like the Surat Basin CSG fields, we cannot assign a source to a plume using $\delta^{13}C_{CH4}$ alone.

Previously, Maher et al. (2014) undertook a mobile CH_4 survey using a Picarro G2201-i CRDS in the Tara region of the Surat Basin. Based on isotopic measurements, they divided the region into a CSG field sub-region (−54.7 ‰) and a non-CSG field

https://doi.org/10.5194/acp-2021-76
Preprint. Discussion started: 5 February 2021


Atmospheric Chemistry and Physics Discussions

sub-region (−47.4 ‰). These results were blended signatures produced by combining all data within each sub-region. As the individual plume analyses shown in Table 2 and Fig 3 demonstrate, single sub-region values cannot be used to isolate CSG emissions from mixtures of other sources, as many sources (CSG, seeps, agricultural) with similar $\delta^{13}C_{CH4}$ signatures co-exist in the CSG sub-region. As shown in this study, attributing CH_4 emissions to CSG sources in the area requires careful analysis using a combination of insights.

Hatch et al. (2018) have also studied CH_4 emissions in the Surat Basin coal seam gas field using a Picarro G2201-i CRDS. The objective of their study was to distinguish between CSG CH_4 (thought initially to be thermogenic origin) and biogenically sourced CH_4. They suggested that $\delta^{13}C_{CH4}$ surveys would not be effective in the Surat Basin, due to small differences of isotopic signatures between the sources of interest. However, our findings are less pessimistic about the usability of $\delta^{13}C_{CH4}$. In the right settings, $\delta^{13}C_{CH4}$ can be used as part of two endmember mixing studies, especially when there are extreme endmembers in the mixed air sample. This is highlighted for the two abattoirs. If the CH_4 emissions downwind of the abattoirs were due to enteric fermentation a $\delta^{13}C_{CH4}$ signature of −63.0 ‰ to −60.0 ‰ would have been recorded. However, at both abattoirs the plumes had isotopic signatures of −46.0 ‰ to −44.0 ‰ (Table 2), so clearly the bulk of the plume being emitted from these facilities is not due to direct cattle emissions and is suspected to be related to the processing of waste meat products, animal wastes, or a mixture of enteric fermentation and biogas combustion. These results highlight the need for further studies on emissions from large feedlots and abattoirs.

This study shows that the combined use of $\delta^{13}C_{CH4}$ and δD_{CH4} provides critical insights into determining the sources of the mapped plumes. In Fig. 3, it is clear that sources such as CSG processing, seeps, ruminants and waste are in distinct dual isotope clusters. In the study area, livestock has relatively depleted $\delta^{13}C_{CH4}$ signatures that are close to CSG sources. However, the δD_{CH4} signatures from cattle, the piggery and the abattoir are 100 ‰ more depleted than the other sources, which successfully sets them apart from CSG sources. We expect the use of $\delta^{13}C_{CH4}$ and δD_{CH4} to reduce uncertainties in interpreting air samples from mixed sources. These results will facilitate improved interpretation of airborne measurements where elevated methane mole fraction readings are due to two or more sources of methane.

Establishing the source signatures for the 17 sources in this study required many weeks in the field and the laboratory. Ensuring statistically robust source signature population statistics in a timely manner requires the development of infield methods. Recent advances in the application of moving Keeling and Miller–Tans methods (Assan et al., 2018; Menoud et al., 2020; Röckmann et al., 2016; Vardag et al., 2016) used in conjunction with portable laser adsorption spectroscopy systems has the potential to provide better source signature population statistics for $\delta^{13}C_{CH4}$ (Kelly and Fisher, 2018; Lu et al., 2019). However, equipment advances are required before we can do in field δD_{CH4} measurements, and as this study has demonstrated both $\delta^{13}C_{CH4}$ and δD_{CH4} are needed for improved source identification. These results also demonstrate the value of collating global databases (Sherwood et al., 2017).

https://doi.org/10.5194/acp-2021-76
Preprint. Discussion started: 5 February 2021

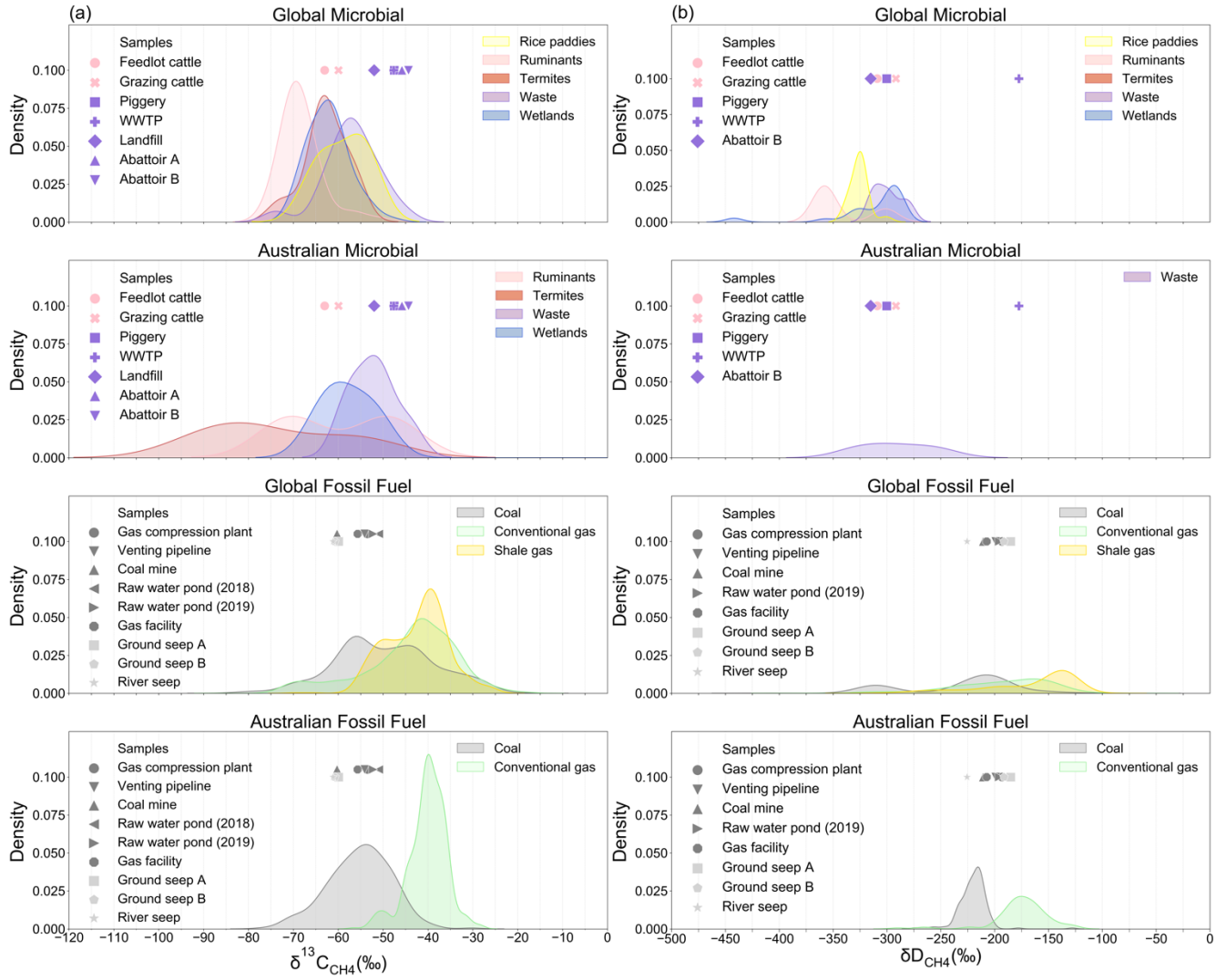

590 **Figure 6: Probability density plot of literature values (globally and from Australia) for (a) $\delta^{13}C_{CH4}$ and (b) δD_{CH4} and results from this study (global values taken from Sherwood et al. (2017) and literature sources listed in Table 1).**

4 Conclusion

In 2018 and 2019, a mobile system was used to map the CH_4 mole fractions and identify various CH_4 sources in the south-eastern Surat Basin coal seam gas fields in Queensland, Australia. Air samples for isotope analysis were collected from CH_4 595 plumes from various sources. The $\delta^{13}C_{CH4}$ and δD_{CH4} signatures of CH_4 emitted from CSG infrastructures, an open-cut coal mine, ground and river seeps, grazing cattle and feedlot, a piggery, a landfill, a wastewater treatment plant, two abattoirs with biogas plants and a small urban area were investigated. Generally, the $\delta^{13}C_{CH4}$ and δD_{CH4} signatures determined from isolated

https://doi.org/10.5194/acp-2021-76
Preprint. Discussion started: 5 February 2021


Atmospheric Chemistry and Physics Discussions

plumes mapped during our 2018 and 2019 campaigns agree with values reported in the literature (Table 1 and Fig. 6). Here we have reported the first recorded $\delta^{13}C_{CH4}$ isotopic signatures of a piggery, two abattoirs, and a wastewater treatment plant in Australia. More investigations in Australia are needed for further characterisation of other sources, both those listed in the UNFCCC inventory classifications and natural. This study has made a contribution to the $\delta^{13}C_{CH4}$ and δD_{CH4} signatures from different sources in Australia and internationally. We also show that the $\delta^{13}C_{CH4}$ and δD_{CH4} signatures of atmospheric CH_4 can provide crucial information for characterising closely located sources. Combined $\delta^{13}C_{CH4}$ and δD_{CH4} signatures separate cattle (both feedlot and pasture) from natural gas seeps and all produced gas sources when measured as unmixed plumes. The dual isotopes $\delta^{13}C_{CH4}$ and δD_{CH4} also separate natural gas seeps, or emissions from the nearer surface portion of the WCM from the production interval within the same coal measure. Results from the piggery and abattoirs cluster together, and these two sources have a $\delta^{13}C_{CH4}$ and δD_{CH4} signature set that is distinct from all other sources sampled.

Previous studies have indicated that using a single tracer (e.g. $\delta^{13}C$) is effective only for single CH_4 emission sources, where a single source is mixed with background air. Challenges emerge when several sources exist in the same region (Hatch et al., 2018; Mielke-Maday et al., 2019; Townsend-Small et al., 2015). Within the Surat Basin the range of $\delta^{13}C_{CH4}$ extends from −63 ‰ to −43 ‰. When considering only $\delta^{13}C_{CH4}$, plumes from abattoirs, piggeries, wastewater treatment plants and conventional gas pipelines cannot be differentiated as to the source mix within these isolated (but multi-source) locations. The $\delta^{13}C_{CH4}$ signatures from coal seam gas sources overlap with signatures expected from landfills. Source attribution using $\delta^{13}C_{CH4}$ signatures alone must be done with local context insights. Without knowing distance to a source or sources, wind speed and direction information, temperature, and mixing layer details, it is not possible from $\delta^{13}C_{CH4}$ signatures alone to separate cattle (both feedlot and pasture) emissions from shallow open-cut coal mines, natural seeps from the upper portion of the Walloon Coal Measures, or many other natural biological sources. However, the distinction of CSG CH_4 emissions is possible using δD_{CH4}, because when it is combined with the $\delta^{13}C_{CH4}$ signature it plots in an isolated cluster in Fig. 3.

It is clear that the separation in the dual isotope plot prompts an in-depth investigation of the feasibility for constraining local and regional-scale emissions. Time series measurements of both $\delta^{13}C_{CH4}$ and δD_{CH4} signatures should also provide further insights for the ongoing rise of the CH_4 mole fraction both regionally and globally.

https://doi.org/10.5194/acp-2021-76
Preprint. Discussion started: 5 February 2021

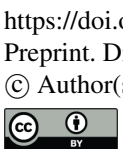

Atmospheric Chemistry and Physics Discussions

Appendix A

Each plume set of air samples (blue dots) were analysed using the Miller–Tans method and the results are shown in Figs A1 – A5. The blue lines are the Bayesian linear regression posterior mean fits, and the 95% highest posterior density intervals (HPDI) are shown in lavender.

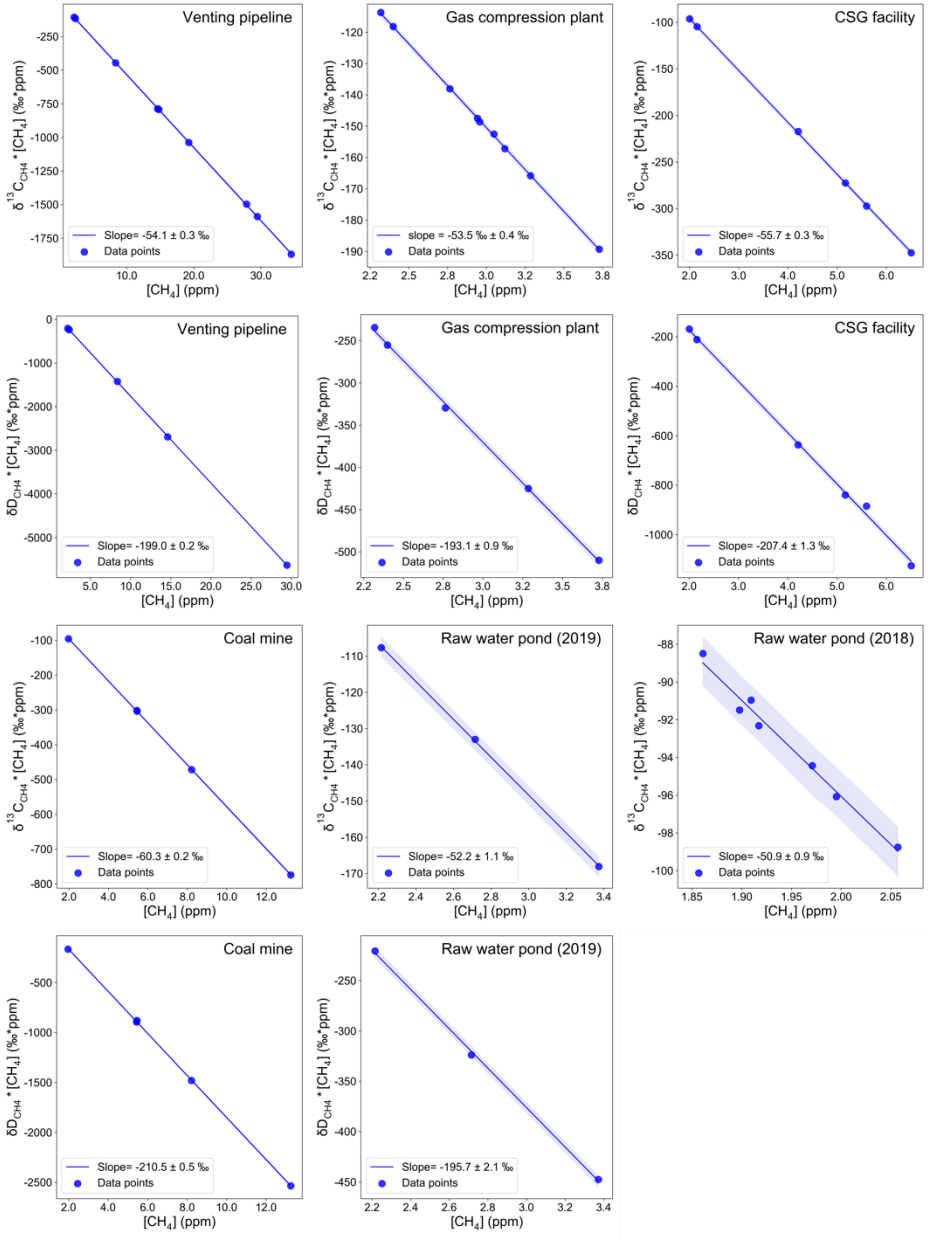

Figure A1: Miller–Tans plots of all data from CSG infrastructures and coal mine using a Bayesian linear regression method. Upper panels show the results for $\delta^{13}C$ and lower panels show the results for δD.

https://doi.org/10.5194/acp-2021-76
Preprint. Discussion started: 5 February 2021

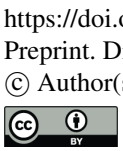

Atmospheric Chemistry and Physics Discussions

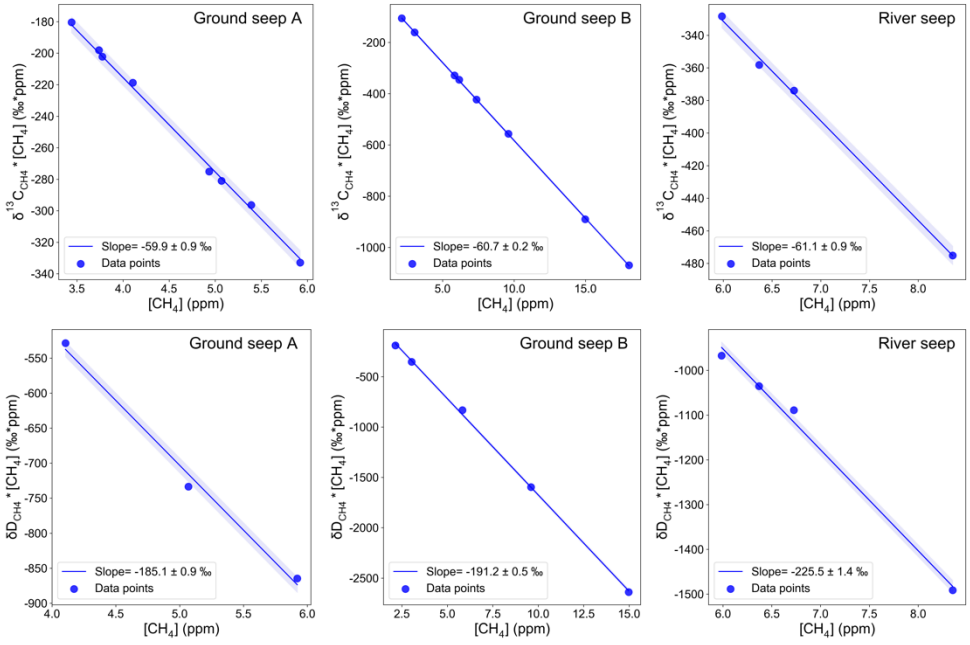

Figure A2: Miller–Tans plots of all data from ground and river seeps using a Bayesian linear regression method. Upper panels show the results for $\delta^{13}C$ and lower panels show the results for δD.

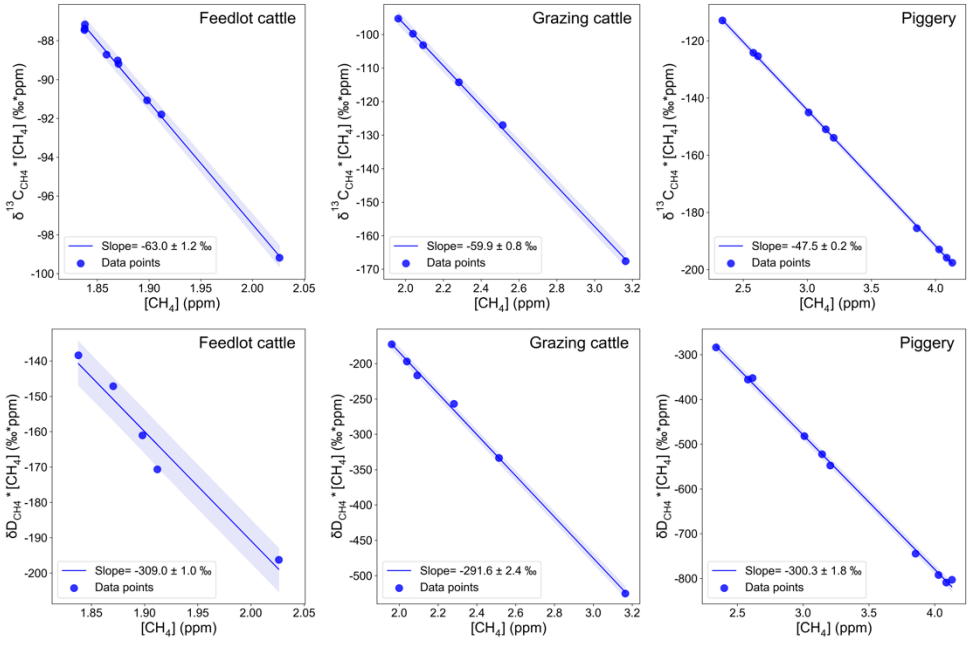

Figure A3: Miller–Tans plots of all data from agriculture sources using a Bayesian linear regression method. Upper panels show the results for $\delta^{13}C$ and lower panels show the results for δD.

https://doi.org/10.5194/acp-2021-76
Preprint. Discussion started: 5 February 2021

Atmospheric Chemistry and Physics Discussions

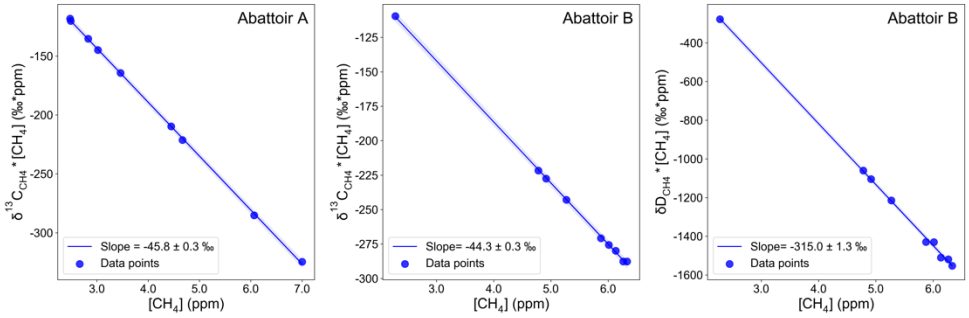

Figure A4: Miller–Tans plots of all data from abattoirs using a Bayesian linear regression method. Left ($\delta^{13}C$) and middle (δD) panels show the results for abattoir A and right panel shows the $\delta^{13}C$ results for abattoir B.

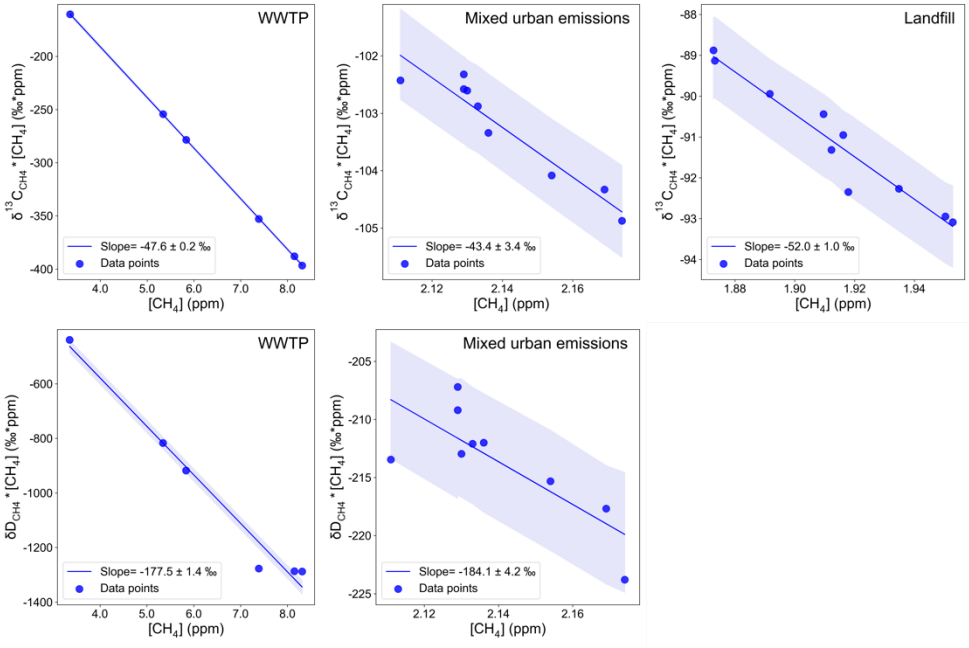

Figure A5: Miller–Tans plots of all data from landfill, WWTP and mixed urban emissions using a Bayesian linear regression method. Upper panels show the results for $\delta^{13}C$ and lower panels show the results for δD.

https://doi.org/10.5194/acp-2021-76
Preprint. Discussion started: 5 February 2021

Atmospheric Chemistry and Physics Discussions

Data availability.

All data are available from the corresponding author upon request.

Author contributions.

Xinyi Lu: Investigation, Formal analysis, Visualisation, Validation, Writing – original draft, Writing – review & editing. Stephen J. Harris: Investigation, Formal analysis, Writing – review & editing. Rebecca E. Fisher: Supervision, Conceptualisation, Methodology, Formal analysis, Writing – review & editing. James L. France: Conceptualisation, Writing – review & editing. Euan G. Nisbet: Conceptualisation, Writing – review & editing. David Lowry: Conceptualisation, Writing – review & editing. Thomas Röckmann: Formal analysis, Writing – review & editing. Carina van der Veen: Formal analysis. Malika Menoud: Formal analysis, Writing – review & editing. Stefan Schwietzke: Conceptualisation, Methodology, Investigation, Validation, Writing – review & editing. Bryce F. J. Kelly: Conceptualisation, Funding acquisition, Supervision, Project administration, Methodology, Validation, Investigation, Formal analysis, Writing – review & editing.

Competing interests.

The authors declare that they have no conflict of interest.

Acknowledgements.

This work was under the support of the Climate and Clean Air Coalition (CCAC) Oil and Gas Methane Science Studies (MSS), hosted by the United Nations Environment Programme. Funding was provided by the Environmental Defense Fund, Oil and Gas Climate Initiative, European Commission and CCAC. The authors thank the MSS Science Advisory Committee, the MSS Technical Working Group as well as Christopher Konek for valuable suggestions and comments on this project. We also thank Bruno Neininger and Jorg Hacker for useful inputs during the field campaign and Lisa Williams for reviewing and editing the final paper. The authors appreciate the insightful feedbacks from the reviewers which helped improving the overall quality of the paper.

Financial support.

The financial support for this study has been provided by Environmental Defense Fund, Oil and Gas Climate Initiative, European Commission and CCAC (United Nations Environment Programme grants DTIE18-EN067 and DTIE19-EN0XX; UNSW grant numbers RG181430 and RG192900). Xinyi Lu is supported in part by UNSW–China Scholarship Council (CSC) Scholarship.

https://doi.org/10.5194/acp-2021-76
Preprint. Discussion started: 5 February 2021

Atmospheric Chemistry and Physics Discussions

680

References

AGL Energy Limited: Agl Fugitive Methane Emissions Monitoring Campaign - Final Report., 2015.

Allen, M. R., Shine, K. P., Fuglestvedt, J. S., Millar, R. J., Cain, M., Frame, D. J. and Macey, A. H.: A solution to the misrepresentations of CO2-equivalent emissions of short-lived climate pollutants under ambitious mitigation, npj Clim. Atmos. Sci., 1(1), 1–8, doi:10.1038/s41612-018-0026-8, 2018.

Assan, S., Vogel, F. R., Gros, V., Baudic, A., Staufer, J. and Ciais, P.: Can we separate industrial CH4 emission sources from atmospheric observations? - A test case for carbon isotopes, PMF and enhanced APCA, Atmos. Environ., 187, 317–327, doi:10.1016/j.atmosenv.2018.05.004, 2018.

Australian Bureau of Statistics: 2016 Census QuickStats: Dalby: https://quickstats.censusdata.abs.gov.au/census_services/getproduct/census/2016/quickstat/SSC30798?opendocument, last access: 31 August 2020.

Australian Bureau of Statistics: 7121.0 - Agricultural Commodities, Australia, 2018-19, 2020.

Australian Competition and Consumer Commission: Gas inquiry 2017-2025 Interim report., 2020.

Australian Government: National Greenhouse Gas Inventory 2019 – UNFCCC classifications: https://ageis.climatechange.gov.au/, last access: 16 June 2020.

Australian Government Clean Energy Regulator: Electricity sector emissions and generation data 2018–19, Natl. Greenh. Energy Report. data, 2020.

Baer, D. S., Paul, J. B., Gupta, M. and O'Keefe, A.: Sensitive absorption measurements in the near-infrared region using off-axis integrated-cavity-output spectroscopy, Appl. Phys. B Lasers Opt., 75(2–3), 261–265, doi:10.1007/s00340-002-0971-z, 2002.

Bakkaloglu, S., Lowry, D., Fisher, R. E., France, J. L., Lanoiselle, M. and Fernandez, J.: Characterization and Quantification of Methane Emissions from Waste in the UK, in EGU General Assembly 2020, Online, pp. EGU2020-12508, EGU General Assembly, Online, 4-8 May., 2020.

Baldwin, S. A. and Larson, M. J.: An introduction to using Bayesian linear regression with clinical data, Behav. Res. Ther., 98, 58–75, doi:10.1016/j.brat.2016.12.016, 2017.

Baublys, K. A., Hamilton, S. K., Golding, S. D., Vink, S. and Esterle, J.: Microbial controls on the origin and evolution of coal seam gases and production waters of the Walloon Subgroup; Surat Basin, Australia, Int. J. Coal Geol., 147–148, 85–104, doi:10.1016/j.coal.2015.06.007, 2015.

Beck, V., Chen, H., Gerbig, C., Bergamaschi, P., Bruhwiler, L., Houweling, S., Rckmann, T., Kolle, O., Steinbach, J., Koch, T., Sapart, C. J., Van Der Veen, C., Frankenberg, C., Andreae, M. O., Artaxo, P., Longo, K. M. and Wofsy, S. C.: Methane airborne measurements and comparison to global models during BARCA, J. Geophys. Res. Atmos., 117(15), doi:10.1029/2011JD017345, 2012.

Beef Central: Qld's Grassdale feedlot completes expansion to 75,000 head: https://www.beefcentral.com/lotfeeding/qlds-grassdale-feedlot-completes-expansion-to-75000-head/, last access: 3 September 2020.

Bilek, R. S., Tyler, S. C., Kurihara, M. and Yagi, K.: Investigation of cattle methane production and emission over a 24-hour period using measurements of δ13C and δD of emitted CH4 and rumen water, J. Geophys. Res. Atmos., 106(D14), 15405–15413, doi:10.1029/2001JD900177, 2001.

BP: BP Statistical Review of World Energy 2019: https://www.bp.com/content/dam/bp/business-sites/en/global/corporate/pdfs/energy-economics/statistical-review/bp-stats-review-2019-full-report.pdf, last access: 27 May 2020.

Brandt, A. R., Heath, G. A. and Cooley, D.: Methane Leaks from Natural Gas Systems Follow Extreme Distributions, Environ. Sci. Technol., 50(22), 12512–12520, doi:10.1021/acs.est.6b04303, 2016.

Brass, M. and Röckmann, T.: Continuous-flow isotope ratio mass spectrometry method for carbon and hydrogen isotope measurements on atmospheric methane, Atmos. Meas. Tech., 3(6), 1707–1721, doi:10.5194/amt-3-1707-2010, 2010.

Brownlow, R., Lowry, D., Fisher, R. E., France, J. L., Lanoisellé, M., White, B., Wooster, M. J., Zhang, T. and Nisbet, E. G.: Isotopic Ratios of Tropical Methane Emissions by Atmospheric Measurement, Global Biogeochem. Cycles, 31(9), 1408–

https://doi.org/10.5194/acp-2021-76
Preprint. Discussion started: 5 February 2021

1419, doi:10.1002/2017GB005689, 2017.

Conley, S., Franco, G., Faloona, I., … D. B.- and 2016, undefined: Methane emissions from the 2015 Aliso Canyon blowout in Los Angeles, CA, science.sciencemag.org, doi:10.1126/science.aac9185, n.d.

Day, C., Tibbett, S., Sestak, A., Knight, S., Marvig, C., Mcgarry, P., Weir, S., White, S., Armand, S., Van Holst, S., Fry, J., Dell'amico, R., Halliburton, M. and Azzi, B.: Methane and Volatile Organic Compound Emissions in New South Wales., 2016.

Day, S., Dell'amico, M., Etheridge, D., Ong, C., Rodger, A., Sherman, B. and Barrett, D. J.: Characterisation of Regional Fluxes of Methane in the Surat Basin, Queensland - Phase 1: A Review and Analysis of Literature on Methane Detection and Flux Determination, Australia., 2013.

Day, S., Dell'Amico, M., Fry, R. and Tousi, H.: Field Measurements of Fugitive Emissions from Equipment and Well Casings in Australian Coal Seam Gas Production Facilities., 2014.

Day, S., Ong, C., Rodger, A., Etheridge, D., Hibberd, M., Van Gorsel, E., Spencer, D., Krummel, P., Zegelin, S., Fry, R., Dell'amico, M., Sestak, S., Williams, D., Zoë, L. and Barrett, D.: Characterisation of Regional Fluxes of Methane in the Surat Basin, Queensland: Phase 2: A pilot study of methodology to detect and quantify methane sources, Australia., 2015.

Department of Natural Resources and Mines: Summary technical report - Part 1: Condamine River gas seep investigation. ., 2012.

Dlugokencky, E. J., Myers, R. C., Lang, P. M., Masarie, K. A., Crotwell, A. M., Thoning, K. W., Hall, B. D., Elkins, J. W. and Steele, L. P.: Conversion of NOAA atmospheric dry air CH4 mole fractions to a gravimetrically prepared standard scale, J. Geophys. Res. D Atmos., 110(18), 1–8, doi:10.1029/2005JD006035, 2005.

Dlugokencky, E. J., Nisbet, E. G., Fisher, R. and Lowry, D.: Global atmospheric methane: Budget, changes and dangers, Philos. Trans. R. Soc. A Math. Phys. Eng. Sci., 369(1943), 2058–2072, doi:10.1098/rsta.2010.0341, 2011.

DNV GL: Energy Transition Outlook 2019 Oil and Gas., 2019.

Doig, A. and Stanmore, P.: The Clarence-Moreton Basin in New South Wales; geology, stratigraphy and coal seam gas characteristics, in Eastern Australasian Basins Symposium IV, Brisbane., 2012.

Draper, J. J. and Boreham, C. J.: Geological Controls On Exploitable Coal Seam Gas Distribution In Queensland, APPEA J., 46(1), 366, doi:10.1071/aj05019, 2006.

EIA: Shale gas production drives world natural gas production growth - Today in Energy - U.S. Energy Information Administration (EIA), 2016.

Etiope, G., Ciotoli, G., Schwietzke, S. and Schoell, M.: Gridded maps of geological methane emissions and their isotopic signature, Earth Syst. Sci. Data, 11(1), 1–22, doi:10.5194/essd-11-1-2019, 2019.

Etminan, M., Myhre, G., Highwood, E. J. and Shine, K. P.: Radiative forcing of carbon dioxide, methane, and nitrous oxide: A significant revision of the methane radiative forcing, Geophys. Res. Lett., 43(24), 12,614-12,623, doi:10.1002/2016GL071930, 2016.

Eyer, S., Tuzson, B., Popa, M. E., van der Veen, C., Röckmann, T., Rothe, M., Brand, W. A., Fisher, R., Lowry, D., Nisbet, E. G., Brennwald, M. S., Harris, E., Zellweger, C., Emmenegger, L., Fischer, H. and Mohn, J.: Real-time analysis of δ^{13}C- and δ D-CH_4 in ambient air with laser spectroscopy: method development and first intercomparison results, Atmos. Meas. Tech., 9(1), 263–280, doi:10.5194/amt-9-263-2016, 2016.

Feinberg, A. I., Coulon, A., Stenke, A., Schwietzke, S. and Peter, T.: Isotopic source signatures: Impact of regional variability on the Δ13CH4 trend and spatial distribution, Atmos. Environ., 174, 99–111, doi:10.1016/j.atmosenv.2017.11.037, 2018.

Fisher, R., Lowry, D., Wilkin, O., Sriskantharajah, S. and Nisbet, E. G.: High-precision, automated stable isotope analysis of atmospheric methane and carbon dioxide using continuous-flow isotope-ratio mass spectrometry, Rapid Commun. Mass Spectrom., 20(2), 200–208, doi:10.1002/rcm.2300, 2006.

Fisher, R. E., Sriskantharajah, S., Lowry, D., Lanoisellé, M., Fowler, C. M. R., James, R. H., Hermansen, O., Lund Myhre, C., Stohl, A., Greinert, J., Nisbet-Jones, P. B. R., Mienert, J. and Nisbet, E. G.: Arctic methane sources: Isotopic evidence for atmospheric inputs, Geophys. Res. Lett., 38(21), doi:10.1029/2011GL049319, 2011.

Fisher, R. E., France, J. L., Lowry, D., Lanoisellé, M., Brownlow, R., Pyle, J. A., Cain, M., Warwick, N., Skiba, U. M., Drewer, J., Dinsmore, K. J., Leeson, S. R., Bauguitte, S. J. -B., Wellpott, A., O'Shea, S. J., Allen, G., Gallagher, M. W., Pitt, J., Percival, C. J., Bower, K., George, C., Hayman, G. D., Aalto, T., Lohila, A., Aurela, M., Laurila, T., Crill, P. M., McCalley, C. K. and Nisbet, E. G.: Measurement of the 13C isotopic signature of methane emissions from northern European wetlands, Global Biogeochem. Cycles, 31(3), 605–623, doi:10.1002/2016GB005504@10.1002/(ISSN)2169-

9291.ARCTICJOINT, 2017.

Flesch, T. K., C Vergé, X. P., Desjardins, R. L. and Worth, D.: Methane emissions from a swine manure tank in western Canada, Can. J. Anim. Sci., 93.1, 159–169, doi:10.4141/CJAS2012-072, 2013.

France, J. L., Cain, M., Fisher, R. E., Lowry, D., Allen, G., O'Shea, S. J., Illingworth, S., Pyle, J., Warwick, N., Jones, B. T., Gallagher, M. W., Bower, K., Le Breton, M., Percival, C., Muller, J., Welpott, A., Bauguitte, S., George, C., Hayman, G. D., Manning, A. J., Myhre, C. L., Lanoisellé, M. and Nisbet, E. G.: Measurements of δ^{13}C in CH_4 and using particle dispersion modeling to characterize sources of Arctic methane within an air mass, J. Geophys. Res. Atmos., 121(23), 14,257-14,270, doi:10.1002/2016JD026006, 2016.

Francey, R. J., L.P. Steele, Spencer, D. A., Langenfelds, R. L., Law, R. M., Krummel, P. B., Fraser, P. J., Etheridge, D. M., Derek, N., Coram, S. A., Cooper, L. N., Allison, C. E. and Porter, L. and B. S.: The CSIRO (Australia) measurement of greenhouse gases in the global atmosphere, Baseline Atmospheric Program (Australia) 1999-2000, Melbourne., 2003.

Fries, A. E., Schifman, L. A., Shuster, W. D. and Townsend-Small, A.: Street-level emissions of methane and nitrous oxide from the wastewater collection system in Cincinnati, Ohio, Environ. Pollut., 236, 247–256, doi:10.1016/j.envpol.2018.01.076, 2018.

Ginty, E. M.: Carbon Isotopic Evidence That Coal Derived Methane Is Altering The Chemistry of The Global Atmosphere, Honours thesis, The University of New South Wales, Australia, 63 pp., 2016.

Golding, S. D., Uysal, I. T., Bolhar, R., Boreham, C. J., Dawson, G. K. W., Baublys, K. A. and Esterle, J. S.: Carbon dioxide-rich coals of the Oaky Creek area, central Bowen Basin: a natural analogue for carbon sequestration in coal systems, Aust. J. Earth Sci., 60(1), 125–140, doi:10.1080/08120099.2012.750627, 2013.

Hamilton, S. K., Esterle, J. S. and Golding, S. D.: Geological interpretation of gas content trends, Walloon Subgroup, eastern Surat Basin, Queensland, Australia, Int. J. Coal Geol., 101, 21–35, doi:10.1016/j.coal.2012.07.001, 2012.

Hamilton, S. K., Golding, S. D., Baublys, K. A. and Esterle, J. S.: Stable isotopic and molecular composition of desorbed coal seam gases from the Walloon Subgroup, eastern Surat Basin, Australia, Int. J. Coal Geol., 122, 21–36, doi:10.1016/j.coal.2013.12.003, 2014.

Hamilton, S. K., Golding, S. D., Baublys, K. A. and Esterle, J. S.: Conceptual exploration targeting for microbially enhanced coal bed methane (MECoM) in the Walloon Subgroup, eastern Surat Basin, Australia, Int. J. Coal Geol., 138, 68–82, doi:10.1016/j.coal.2014.12.002, 2015.

Hatch, M. A., Kennedy, M. J., Hamilton, M. W. and Vincent, R. A.: Methane variability associated with natural and anthropogenic sources in an Australian context, Aust. J. Earth Sci., 65(5), 683–690, doi:10.1080/08120099.2018.1471004, 2018.

Hausmann, P., Sussmann, R. and Smale, D.: Contribution of oil and natural gas production to renewed increase in atmospheric methane (2007–2014): top–down estimate from ethane and methane column observations, Atmos. Chem. Phys., 16(5), 3227–3244, doi:10.5194/acp-16-3227-2016, 2016.

Hmiel, B., Petrenko, V. V., Dyonisius, M. N., Buizert, C., Smith, A. M., Place, P. F., Harth, C., Beaudette, R., Hua, Q., Yang, B., Vimont, I., Michel, S. E., Severinghaus, J. P., Etheridge, D., Bromley, T., Schmitt, J., Faïn, X., Weiss, R. F. and Dlugokencky, E.: Preindustrial 14CH4 indicates greater anthropogenic fossil CH4 emissions, Nature, 578(7795), 409–412, doi:10.1038/s41586-020-1991-8, 2020.

Hoheisel, A., Yeman, C., Dinger, F., Eckhardt, H. and Schmidt, M.: An improved method for mobile characterisation of $\delta^{13}$$CH_4$ source signatures and its application in Germany, Atmos. Meas. Tech., 12(2), 1123–1139, doi:10.5194/amt-12-1123-2019, 2019.

IEA: Key World Energy Statistics: https://www.iea.org/reports/key-world-energy-statistics-2019, last access: 18 May 2020.

Iverach, C. P., Lowry, D., France, J. L., Fisher, R. E., Nisbet, E. G., Baker, A., Acworth, R. I., Loh, Z., Day, S. and Kelly, B. F. J.: The Complexities of Continuous Air Monitoring in Attributing Methane to Sources of Production, in Australian Earth Science Convention, Newcastle, Australia, 7–10 July 2014, pp. 17–18., 2014.

Iverach, C. P., Cendón, D. I., Hankin, S. I., Lowry, D., Fisher, R. E., France, J. L., Nisbet, E. G., Baker, A. and Kelly, B. F. J.: Assessing Connectivity Between an Overlying Aquifer and a Coal Seam Gas Resource Using Methane Isotopes, Dissolved Organic Carbon and Tritium, Sci. Rep., 5(1), 1–11, doi:10.1038/srep15996, 2015.

Iverach, C. P., Beckmann, S., Cendón, D. I., Manefield, M. and Kelly, B. F. J.: Biogeochemical constraints on the origin of methane in an alluvial aquifer: evidence for the upward migration of methane from underlying coal measures, Biogeosciences, 14(1), 215–228, doi:10.5194/bg-14-215-2017, 2017.

https://doi.org/10.5194/acp-2021-76
Preprint. Discussion started: 5 February 2021

Atmospheric Chemistry and Physics Discussions

Jackson, R. B., Saunois, M., Bousquet, P., Canadell, J. G., Poulter, B., Stavert, A. R., Bergamaschi, P., Niwa, Y., Segers, A. and Tsuruta, A.: Increasing anthropogenic methane emissions arise equally from agricultural and fossil fuel sources, Environ. Res. Lett., 15(7), 071002, doi:10.1088/1748-9326/ab9ed2, 2020.

Jaynes, E. T. and Crow, W.: Straight Line Fitting - A Bayesian Solution, Unpubl. Manuscr., item 22, 1999.

Joos, F., Roth, R., Fuglestvedt, J. S., Peters, G. P., Enting, I. G., Von Bloh, W., Brovkin, V., Burke, E. J., Eby, M., Edwards, N. R., Friedrich, T., Frölicher 11, T. L., Halloran, P. R., Holden, P. B., Jones, C., Kleinen, T., Mackenzie, F. T., Matsumoto, K., Meinshausen, M., Plattner, G.-K., Reisinger, A., Segschneider, J., Shaffer, G., Steinacher, M., Strassmann, K., Tanaka, K., Timmermann, A. and Weaver, A. J.: Carbon dioxide and climate impulse response functions for the computation of greenhouse gas metrics: a multi-model analysis, Atmos. Chem. Phys, 13, 2793–2825, doi:10.5194/acp-13-2793-2013, 2013.

Keeling, C. D.: The concentration and isotopic abundances of atmospheric carbon dioxide in rural areas, Geochim. Cosmochim. Acta, 13(4), 322–334, doi:10.1016/0016-7037(58)90033-4, 1958.

Kelly, B. F. J. and Fisher, R. E.: Continuous Tracking of Air Parcel Mixing Using Discrete Wavelet Transformation of Urban Ground Level Atmospheric Methane Measurements, in Geophysical Research Abstracts, vol. 20, pp. EGU2018-6265–1, EGU General Assembly, Vienna, Austria, 8-13 April., 2018.

Kelly, B. F. J. and Iverach, C. P.: River on fire: even if it's not coal seam gas we should still be concerned, Conversat., 3rd May 2016: https://theconversation.com/river-on-fire-even-if-its-not-coal-seam-gas-we-should-still-be-concerned-58718, last access: 27 May 2020.

Kelly, B. F. J., Iverach, C. P., Lowry, D., Fisher, R. E., France, J. L. and Nisbet, E. G.: Fugitive methane emissions from natural, urban, agricultural, and energy-production landscapes of eastern Australia., 2015a.

Kelly, B. F. J., Iverach, C. P., Lowry, D., Fisher, R. E., France, J. L. and Nisbet, E. G.: Fugitive methane emissions from natural, urban, agricultural, and energy-production landscapes of eastern Australia, in Geophysical Research Abstracts, vol. 17, pp. EGU2015-5135, EGU General Assembly, Vienna, Austria, 12-17 April., 2015b.

Kelly, B. F. J., Iverach, C. P., Ginty, E., Bashir, S., Lowry, D., Fisher, R. E., France, J. L. and Nisbet, E. G.: The case for refining bottom-up methane emission inventories using top-down measurements, in Geophysical Research Abstracts, vol. 19, pp. EGU2017-5700, EGU General Assembly, Vienna, Austria, 23-28 April., 2017.

Kille, N., Chiu, R., Frey, M., Hase, F., Sha, M. K., Blumenstock, T., Hannigan, J. W., Orphal, J., Bon, D. and Volkamer, R.: Separation of Methane Emissions From Agricultural and Natural Gas Sources in the Colorado Front Range, Geophys. Res. Lett., 46(7), 3990–3998, doi:10.1029/2019GL082132, 2019.

Kirschke, S., Bousquet, P., Ciais, P., Saunois, M., Canadell, J. G., Dlugokencky, E. J., Bergamaschi, P., Bergmann, D., Blake, D. R., Bruhwiler, L., Cameron-Smith, P., Castaldi, S., Chevallier, F., Feng, L., Fraser, A., Heimann, M., Hodson, E. L., Houweling, S., Josse, B., Fraser, P. J., Krummel, P. B., Lamarque, J.-F., Langenfelds, R. L., Le Quéré, C., Naik, V., Palmer, P. I., Pison, I., Plummer, D., Poulter, B., Prinn, R. G., Rigby, M., Ringeval, B., Santini, M., Schmidt, M., Shindell, D. T., Simpson, I. J., Spahni, R., Paul Steele, L., Strode, S. A., Sudo, K., Szopa, S., van der Werf, G. R., Voulgarakis, A., van Weele, M., Weiss, R. F., Williams, J. E. and Zeng, G.: Three decades of global methane sources and sinks, Nat. Publ. Gr., 6, doi:10.1038/NGEO1955, 2013.

Lan, X., Tans, P., Sweeney, C., Andrews, A., Dlugokencky, E., Schwietzke, S., Kofler, J., McKain, K., Thoning, K., Crotwell, M., Montzka, S., Miller, B. R. and Biraud, S. C.: Long-Term Measurements Show Little Evidence for Large Increases in Total U.S. Methane Emissions Over the Past Decade, Geophys. Res. Lett., 46(9), 4991–4999, doi:10.1029/2018GL081731, 2019.

Levin, I., Bergamaschi, P., Dörr, H. and Trapp, D.: Stable isotopic signature of methane from major sources in Germany, Chemosphere, 26(1–4), 161–177, doi:10.1016/0045-6535(93)90419-6, 1993.

Lowry, D., Fisher, R. E., France, J. L., Coleman, M., Lanoisellé, M., Zazzeri, G., Nisbet, E. G., Shaw, J. T., Allen, G., Pitt, J. and Ward, R. S.: Environmental baseline monitoring for shale gas development in the UK: Identification and geochemical characterisation of local source emissions of methane to atmosphere, Sci. Total Environ., 708, 134600, doi:10.1016/j.scitotenv.2019.134600, 2020.

Lu, X., Iverach, C. P., Harris, S. J., Fisher, R. E., Lowry, D., France, J. L., Nisbet, E. G., Loh, Z. M., Phillips, F., Schwietzke, S., Hacker, J., Neininger, B. and Kelly, B. F. J.: In Plume Miller-Tans Time Series Analyses for Improved Isotopic Source Signature Characterisation, in Geophysical Research Abstracts, vol. 21, pp. EGU2019-11559–1, EGU General Assembly, Vienna, Austria, 7-12 April., 2019.

https://doi.org/10.5194/acp-2021-76
Preprint. Discussion started: 5 February 2021

Lu, X., Harris, S. J., Fisher, R. E., Lowry, D., France, J. L., Hacker, J., Neininger, B., Röckmann, T., van der Veen, C., Menoud, M., Schwietzke, S. and Kelly, B. F. J.: Methane Source Attribution Challenges in the Surat Basin, Australia, in EGU General Assembly 2020, Online, pp. EGU2020-12508, EGU General Assembly,Online, 4-8 May., 2020.

Luhar, A., Etheridge, D., Loh, Z., Noonan, N., Spencer, D. and Day, S.: Characterisation of Regional Fluxes of Methane in the Surat Basin, Queensland. Final report on Task 3: Broad scale application of methane detection, and Task 4: Methane emissions enhanced modelling, Report to the Gas Industry Social and Environmental Research Alliance (GISERA). Report No. EP185211,., 2018.

Luhar, A. K., Etheridge, D. M., Loh, Z. M., Noonan, J., Spencer, D., Smith, L. and Ong, C.: Quantifying methane emissions from Queensland's coal seam gas producing Surat Basin using inventory data and a regional Bayesian inversion, Atmos. Chem. Phys., 20(23), 15487–15511, doi:10.5194/acp-20-15487-2020, 2020.

Maazallahi, H., Fernandez, J. M., Menoud, M., Zavala-Araiza, D., Weller, Z. D., Schwietzke, S., von Fischer, J. C., Denier van der Gon, H. and Röckmann, T.: Methane mapping, emission quantification, and attribution in two European cities: Utrecht (NL) and Hamburg (DE), Atmos. Chem. Phys., 20(23), 14717–14740, doi:10.5194/acp-20-14717-2020, 2020.

Maher, D. T., Santos, I. R. and Tait, D. R.: Mapping methane and carbon dioxide concentrations and δ13c values in the atmosphere of two Australian coal seam gas fields, Water. Air. Soil Pollut., 225(12), 1–9, doi:10.1007/s11270-014-2216-2, 2014.

Maher, D. T., Cowley, K., Santos, I. R., Macklin, P. and Eyre, B. D.: Methane and carbon dioxide dynamics in a subtropical estuary over a diel cycle: Insights from automated in situ radioactive and stable isotope measurements, Mar. Chem., 168, 69–79, doi:10.1016/j.marchem.2014.10.017, 2015.

McGinn, S. M., Chen, D., Loh, Z., Hill, J., Beauchemin, K. A. and Denmead, O. T.: Methane emissions from feedlot cattle in Australia and Canada, Aust. J. Exp. Agric., 48(2), 183, doi:10.1071/EA07204, 2008.

McGlade, C., Speirs, J. and Sorrell, S.: Unconventional gas - A review of regional and global resource estimates, Energy, 55, 571–584, doi:10.1016/j.energy.2013.01.048, 2013.

McNorton, J., Wilson, C., Gloor, M., Parker, R. J., Boesch, H., Feng, W., Hossaini, R. and Chipperfield, M. P.: Attribution of recent increases in atmospheric methane through 3-D inverse modelling, Atmos. Chem. Phys., 18(24), 18149–18168, doi:10.5194/acp-18-18149-2018, 2018.

Menoud, M., van der Veen, C., Scheeren, B., Chen, H., Szénási, B., Morales, R. P., Pison, I., Bousquet, P., Brunner, D. and Röckmann, T.: Characterisation of methane sources in Lutjewad, The Netherlands, using quasi-continuous isotopic composition measurements, Tellus, Ser. B Chem. Phys. Meteorol., 72(1), 1–19, doi:10.1080/16000889.2020.1823733, 2020.

Mielke-Maday, I., Schwietzke, S., Yacovitch, T., Miller, B., Conley, S., Kofler, J., Handley, P., Thorley, E., Herndon, S. C., Hall, B., Dlugokencky, E., Lang, P., Wolter, S., Moglia, E., Crotwell, M., Crotwell, A., Rhodes, M., Kitzis, D., Vaughn, T., Bell, C., Zimmerle, D., Schnell, R. and Pétron, G.: Methane source attribution in a U.S. dry gas basin using spatial patterns of ground and airborne ethane and methane measurements, Elem Sci Anth, 7(1), 13, doi:10.1525/elementa.351, 2019.

Milkov, A. V. and Etiope, G.: Revised genetic diagrams for natural gases based on a global dataset of >20,000 samples, Org. Geochem., 125, 109–120, doi:10.1016/j.orggeochem.2018.09.002, 2018.

Miller, J. B. and Tans, P. P.: Calculating isotopic fractionation from atmospheric measurements at various scales, Tellus B, 55(2), 207–214, doi:10.1034/j.1600-0889.2003.00020.x, 2003.

Monteny, G. J., Bannink, A. and Chadwick, D.: Greenhouse gas abatement strategies for animal husbandry, in Agriculture, Ecosystems and Environment, vol. 112, pp. 163–170, Elsevier., 2006.

Myhre, G., Shindell, D., Bréon F.-M., Collins, W., Fuglestvedt, J., Huang, J., Koch, D., Lamarque, J.-F., Lee, D., Mendoza, B., Nakajima, T., Robock, A., Stephens, G., Takemura, T. and H.Zhang: Anthropogenic and natural radiative forcing, in Climate Change 2013 the Physical Science Basis: Working Group I Contribution to the Fifth Assessment Report of the Intergovernmental Panel on Climate Change, vol. 9781107057, edited by Intergovernmental Panel on Climate Change, pp. 659–740, Cambridge University Press, Cambridge, United Kingdom and New York, NY, USA., 2013.

NH Foods: Oakey Beef Exports: https://www.nh-foods.com.au/facilities/oakey-beef-exports/, last access: 4 September 2020).

Nisbet, E. G., Dlugokencky, E. J. and Bousquet, P.: Methane on the rise - Again, Science (80-.)., 343(6170), 493–495, doi:10.1126/science.1247828, 2014.

Nisbet, E. G., Dlugokencky, E. J., Manning, M. R., Lowry, D., Fisher, R. E., France, J. L., Michel, S. E., Miller, J. B., White,

J. W. C., Vaughn, B., Bousquet, P., Pyle, J. A., Warwick, N. J., Cain, M., Brownlow, R., Zazzeri, G., Lanoisellé, M., Manning, A. C., Gloor, E., Worthy, D. E. J., Brunke, E.-G., Labuschagne, C., Wolff, E. W. and Ganesan, A. L.: Rising atmospheric methane: 2007-2014 growth and isotopic shift, Global Biogeochem. Cycles, 30(9), 1356–1370, doi:10.1002/2016GB005406, 2016.

Nisbet, E. G., Manning, M. R., Dlugokencky, E. J., Fisher, R. E., Lowry, D., Michel, S. E., Myhre, C. L., Platt, S. M., Allen, G., Bousquet, P., Brownlow, R., Cain, M., France, J. L., Hermansen, O., Hossaini, R., Jones, A. E., Levin, I., Manning, A. C., Myhre, G., Pyle, J. A., Vaughn, B. H., Warwick, N. J. and White, J. W. C.: Very Strong Atmospheric Methane Growth in the 4 Years 2014–2017: Implications for the Paris Agreement, Global Biogeochem. Cycles, 33(3), 318–342, doi:10.1029/2018GB006009, 2019.

Nisbet, E. G., Fisher, R. E., Lowry, D., France, J. L., Allen, G., Bakkaloglu, S., Broderick, T. J., Cain, M., Coleman, M., Fernandez, J., Forster, G., Griffiths, P. T., Iverach, C. P., Kelly, B. F. J., Manning, M. R., Nisbet-Jones, P. B. R., Pyle, J. A., Townsend-Small, A., al-Shalaan, A., Warwick, N. and Zazzeri, G.: Methane Mitigation: Methods to Reduce Emissions, on the Path to the Paris Agreement, Rev. Geophys., 58(1), doi:10.1029/2019RG000675, 2020.

Obersky, L., Rafiee, R., Cabral, A. R., Golding, S. D. and Clarke, W. P.: Methodology to determine the extent of anaerobic digestion, composting and CH4 oxidation in a landfill environment, Waste Manag., 76, 364–373, doi:10.1016/j.wasman.2018.02.029, 2018.

Owen, D. D. R., Shouakar-Stash, O., Morgenstern, U. and Aravena, R.: Thermodynamic and hydrochemical controls on CH4 in a coal seam gas and overlying alluvial aquifer: New insights into CH4 origins, Sci. Rep., 6(1), 1–20, doi:10.1038/srep32407, 2016.

Pallasser, R. and Stalker, L.: Dissolved Gas Measurements For Bores In The South Eastern Part Of The Surat Basin (Great Artesian Basin, North Eastern Nsw). A report to the NSW Department of Mineral Resources., 2001.

QGC: QGC Stage 3 Water Monitoring and Management Plan. Chapter 14.0:Associated water management., 2014.

Queensland Government: Queensland Spatial Catalogue - Qspatial: http://qldspatial.information.qld.gov.au/catalogue/custom/detail.page?fid=%7B30B884DA-4B6C-4129-9081-32525DA3143C%7D, last access: 3 September 2020.

Queensland Government: Queensland Spatial Catalogue - QSpatial: http://qldspatial.information.qld.gov.au/catalogue/custom/detail.page?fid=%7BB443A9EE-861C-46BC-AE7C-D2E023E477EA%7D, last access: Accessed 3 September 2020.

Queensland Government: Coal industry review statistical tables - Production of saleable coal by individual mines | Open Data Portal | Queensland Government: https://www.data.qld.gov.au/dataset/coal-industry-review-statistical-tables/resource/1b7fb643-c880-42bf-940b-fc3c582d239d, last access: 26 May 2020).

Queensland Government: Petroleum and gas production and reserve statistics, Open Data Portal: https://www.data.qld.gov.au/dataset/petroleum-gas-production-and-reserve-statistics, last access: 16 June 2020.

Queensland Government: Queensland borehole series - All bore hole and well locations - Queensland | Open Data Portal | Queensland Government, All bore hole well Location - Queensland: https://www.data.qld.gov.au/dataset/queensland-borehole-series/resource/74c36af5-f924-4d45-bf89-e6673bcd13e2, last access: 26 May 2020.

Queensland Government: Queensland Globe | Business Queensland: https://www.business.qld.gov.au/running-business/support-assistance/mapping-data-imagery/queensland-globe, last access: 22 June 2020.

Rice, A. L., Butenhoff, C. L., Teama, D. G., Röger, F. H., Khalil, M. A. K. and Rasmussen, R. A.: Atmospheric methane isotopic record favors fossil sources flat in 1980s and 1990s with recent increase, Proc. Natl. Acad. Sci. U. S. A., 113(39), 10791–10796, doi:10.1073/pnas.1522923113, 2016.

Rigby, M., Montzka, S. A., Prinn, R. G., White, J. W. C., Young, D., O'Doherty, S., Lunt, M. F., Ganesan, A. L., Manning, A. J., Simmonds, P. G., Salameh, P. K., Harth, C. M., Mühle, J., Weiss, R. F., Fraser, P. J., Steele, L. P., Krummel, P. B., McCulloch, A. and Park, S.: Role of atmospheric oxidation in recent methane growth, Proc. Natl. Acad. Sci. U. S. A., 114(21), 5373–5377, doi:10.1073/pnas.1616426114, 2017.

Röckmann, T., Eyer, S., Van Der Veen, C., Popa, M. E., Tuzson, B., Monteil, G., Houweling, S., Harris, E., Brunner, D., Fischer, H., Zazzeri, G., Lowry, D., Nisbet, E. G., Brand, W. A., Necki, J. M., Emmenegger, L. and Mohn, J.: In situ observations of the isotopic composition of methane at the Cabauw tall tower site, Atmos. Chem. Phys, 16, 10469–10487, doi:10.5194/acp-16-10469-2016, 2016.

Rosentreter, J. A., Maher, D. T., Erler, D. V., Murray, R. and Eyre, B. D.: Factors controlling seasonal CO2 and CH4 emissions

https://doi.org/10.5194/acp-2021-76
Preprint. Discussion started: 5 February 2021

in three tropical mangrove-dominated estuaries in Australia, Estuar. Coast. Shelf Sci., 215, 69–82, doi:10.1016/j.ecss.2018.10.003, 2018.

Salvatier, J., Wiecki, T. V. and Fonnesbeck, C.: Probabilistic programming in Python using PyMC3, PeerJ Comput. Sci., 2016(4), e55, doi:10.7717/peerj-cs.55, 2016.

Saunois, M., Bousquet, P., Poulter, B., Peregon, A., Ciais, P., Canadell, J. G., Dlugokencky, E. J., Etiope, G., Bastviken, D., Houweling, S., Janssens-Maenhout, G., Tubiello, F. N., Castaldi, S., Jackson, R. B., Alexe, M., Arora, V. K., Beerling, D. J., Bergamaschi, P., Blake, D. R., Brailsford, G., Brovkin, V., Bruhwiler, L., Crevoisier, C., Crill, P., Covey, K., Curry, C., Frankenberg, C., Gedney, N., Höglund-Isaksson, L., Ishizawa, M., Ito, A., Joos, F., Kim, H. S., Kleinen, T., Krummel, P., Lamarque, J. F., Langenfelds, R., Locatelli, R., Machida, T., Maksyutov, S., McDonald, K. C., Marshall, J., Melton, J. R., Morino, I., Naik, V., O'Doherty, S., Parmentier, F. J. W., Patra, P. K., Peng, C., Peng, S., Peters, G. P., Pison, I., Prigent, C., Prinn, R., Ramonet, M., Riley, W. J., Saito, M., Santini, M., Schroeder, R., Simpson, I. J., Spahni, R., Steele, P., Takizawa, A., Thornton, B. F., Tian, H., Tohjima, Y., Viovy, N., Voulgarakis, A., Van Weele, M., Van Der Werf, G. R., Weiss, R., Wiedinmyer, C., Wilton, D. J., Wiltshire, A., Worthy, D., Wunch, D., Xu, X., Yoshida, Y., Zhang, B., Zhang, Z. and Zhu, Q.: The global methane budget 2000-2012, Earth Syst. Sci. Data, 8(2), 697–751, doi:10.5194/essd-8-697-2016, 2016.

Schaefer, H., Fletcher, S. E. M., Veidt, C., Lassey, K. R., Brailsford, G. W., Bromley, T. M., Dlugokencky, E. J., Michel, S. E., Miller, J. B., Levin, I., Lowe, D. C., Martin, R. J., Vaughn, B. H. and White, J. W. C.: A 21st-century shift from fossil-fuel to biogenic methane emissions indicated by 13CH4, Science (80-.)., 352(6281), 80–84, doi:10.1126/science.aad2705, 2016.

Schwietzke, S., Griffin, W. M., Matthews, H. S. and Bruhwiler, L. M. P.: Natural gas fugitive emissions rates constrained by global atmospheric methane and ethane, Environ. Sci. Technol., 48(14), 7714–7722, doi:10.1021/es501204c, 2014.

Schwietzke, S., Sherwood, O. A., Bruhwiler, L. M. P., Miller, J. B., Etiope, G., Dlugokencky, E. J., Michel, S. E., Arling, V. A., Vaughn, B. H., White, J. W. C. and Tans, P. P.: Upward revision of global fossil fuel methane emissions based on isotope database, Nature, 538(7623), 88–91, doi:10.1038/nature19797, 2016.

Sherwood, O., Schwietzke, S., Arling, V. and Etiope, G.: Global Inventory of Fossil and Non-fossil Methane δ13C Source Signature Measurements for Improved Atmospheric Modeling, NOAA, doi:10.15138/G37P4D, 2016.

Sherwood, O. A., Schwietzke, S., Arling, V. A. and Etiope, G.: Global Inventory of Gas Geochemistry Data from Fossil Fuel, Microbial and Burning Sources, version 2017, Earth Syst. Sci. Data, 9, 639–656, doi:10.5194/essd-9-639-2017, 2017.

Smith, M. L., Kort, E. A., Karion, A., Sweeney, C., Herndon, S. C. and Yacovitch, T. I.: Airborne Ethane Observations in the Barnett Shale: Quantification of Ethane Flux and Attribution of Methane Emissions, Environ. Sci. Technol., 49(13), 8158–8166, doi:10.1021/acs.est.5b00219, 2015.

Stieger, J., Bamberger, I., Buchmann, N. and Eugster, W.: Validation of farm-scale methane emissions using nocturnal boundary layer budgets, Atmos. Chem. Phys, 15, 14055–14069, doi:10.5194/acp-15-14055-2015, 2015.

Sugimoto, A., Inoue, T., Tayasu, I., Miller, L., Takeichi, S. and Abe, T.: Methane and hydrogen production in a termite-symbiont system, Ecol. Res., 13(2), 241–257, doi:10.1046/j.1440-1703.1998.00262.x, 1998.

Tarasova, O. A., Brenninkmeijer, C. A. M., Assonov, S. S., Elansky, N. F., Röckmann, T. and Brass, M.: Atmospheric CH4 along the Trans-Siberian railroad (TROICA) and river Ob: Source identification using stable isotope analysis, Atmos. Environ., 40(29), 5617–5628, doi:10.1016/j.atmosenv.2006.04.065, 2006.

Towler, B., Firouzi, M., Underschultz, J., Rifkin, W., Garnett, A., Schultz, H., Esterle, J., Tyson, S. and Witt, K.: An overview of the coal seam gas developments in Queensland, , doi:10.1016/j.jngse.2016.02.040, 2016.

Townsend-Small, A., Tyler, S. C., Pataki, D. E., Xu, X. and Christensen, L. E.: Isotopic measurements of atmospheric methane in Los Angeles, California, USA: Influence of "fugitive" fossil fuel emissions, J. Geophys. Res. Atmos., 117(7), doi:10.1029/2011JD016826, 2012.

Townsend-Small, A., Marrero, J. E., Lyon, D. R., Simpson, I. J., Meinardi, S. and Blake, D. R.: Integrating Source Apportionment Tracers into a Bottom-up Inventory of Methane Emissions in the Barnett Shale Hydraulic Fracturing Region, Environ. Sci. Technol., 49(13), 8175–8182, doi:10.1021/acs.est.5b00057, 2015.

Townsend-Small, A., Botner, E. C., Jimenez, K. L., Schroeder, J. R., Blake, N. J., Meinardi, S., Blake, D. R., Sive, B. C., Bon, D., Crawford, J. H., Pfister, G. and Flocke, F. M.: Using stable isotopes of hydrogen to quantify biogenic and thermogenic atmospheric methane sources: A case study from the Colorado Front Range, Geophys. Res. Lett., 43(21), 11,462-11,471, doi:10.1002/2016GL071438, 2016.

https://doi.org/10.5194/acp-2021-76
Preprint. Discussion started: 5 February 2021

Atmospheric Chemistry and Physics Discussions

Toyoda, S., Suzuki, Y., Hattori, S., Yamada, K., Fujii, A., Yoshida, N., Kouno, R., Murayama, K. and Shiomi, H.: Isotopomer analysis of production and consumption mechanisms of N 2O and CH4 in an advanced wastewater treatment system, Environ. Sci. Technol., 45(3), 917–922, doi:10.1021/es102985u, 2011.

Tsai, T. R., Du, K. and Stavropoulos, B.: New system for detecting, mapping, monitoring, quantifying and reporting fugitive gas emissions, APPEA J., 57(2), 561, doi:10.1071/aj16098, 2017.

Turner, A. J., Frankenberg, C., Wennberg, P. O. and Jacob, D. J.: Ambiguity in the causes for decadal trends in atmospheric methane and hydroxyl, Proc. Natl. Acad. Sci. U. S. A., 114(21), 5367–5372, doi:10.1073/pnas.1616020114, 2017.

Vardag, S. N., Hammer, S. and Levin, I.: Evaluation of 4 years of continuous δ 13 C(CO 2) data using a moving Keeling plot method, Biogeosciences, 13, 4237–4251, doi:10.5194/bg-13-4237-2016, 2016.

White, J. W. C., B. H. Vaughn and S. E. Michel: University of Colorado, Institute of Arctic and Alpine Research (INSTAAR), Stable Isotopic Composition of Atmospheric Methane (13C) from the NOAA ESRL Carbon Cycle Cooperative Global Air Sampling Network, 1998-2017, Version: 2018-09-24: ftp://aftp.cmdl.noaa.gov/data/trace_gases/ch4c13/flask/, 2018.

Worden, J. R., Bloom, A. A., Pandey, S., Jiang, Z., Worden, H. M., Walker, T. W., Houweling, S. and Röckmann, T.: Reduced biomass burning emissions reconcile conflicting estimates of the post-2006 atmospheric methane budget, Nat. Commun., 8(1), 1–11, doi:10.1038/s41467-017-02246-0, 2017.

Xueref-Remy, I., Zazzeri, G., Bréon, F. M., Vogel, F., Ciais, P., Lowry, D. and Nisbet, E. G.: Anthropogenic methane plume detection from point sources in the Paris megacity area and characterization of their δ13C signature, Atmos. Environ., 222, 117055, doi:10.1016/j.atmosenv.2019.117055, 2020.

Yancoal: Environmental Assessment Cameby Downs Continued Operations Project., 2018.

Zazzeri, G.: Methane Emissions in UK: Deciphering Regional Sources with Mobile Measurements and Isotopic Characterisation, Ph.D. thesis, Royal Holloway, University of London, UK, 264 pp., 2016.

Zazzeri, G., Lowry, D., Fisher, R. E., France, J. L., Lanoisellé, M. and Nisbet, E. G.: Plume mapping and isotopic characterisation of anthropogenic methane sources, Atmos. Environ., 110, 151–162, doi:10.1016/j.atmosenv.2015.03.029, 2015.

Zazzeri, G., Lowry, D., Fisher, R. E., France, J. L., Lanoisellé, M., Kelly, B. F. J., Necki, J. M., Iverach, C. P., Ginty, E., Zimnoch, M., Jasek, A. and Nisbet, E. G.: Carbon isotopic signature of coal-derived methane emissions to the atmosphere: from coalification to alteration, Atmos. Chem. Phys, 16, 13669–13680, doi:10.5194/acp-16-13669-2016, 2016.